Building blocks for the chemistry of perfluorinated alkoxyaluminates $[Al\{OC(CF_3)_3\}_4]^-$: simplified preparation and characterization of Li^+–Cs^+, Ag^+, NH_4^+, $N_2H_5^+$ and $N_2H_7^+$ salts

Electronic Supplementary Information

Przemysław J. Malinowski,[a]* Tomasz Jaroń,[a]* Małgorzata Domańska,[b] John Slattery,[c] Manuel Schmitt,[d] and Ingo Krossing[d]

[a] Centre of New Technologies, University of Warsaw, Banacha 2c, 02-097 Warsaw, Poland.
[b] Faculty of Physics, University of Warsaw, Pasteura 5,02-093 Warsaw, Poland.
[c] Department of Chemistry, University of York, Heslington, York YO10 5DD, United Kingdom.
[d] Institut für Anorganische und Analytische Chemie and Freiburger Materialforschungszentrum (FMF), Universität Freiburg, Albertstr. 21, 79104 Freiburg, Germany.
* Correspondence to malin@cent.uw.edu.pl and t.jaron@cent.uw.edu.pl

Table of contents

1. Experimental methods

1.1. Synthetic procedures

Typically, all manipulations have been performed in argon atmosphere in MBraun gloveboxes (typically <1 ppm O_2 and <1 ppm H_2O) or in Schlenk-type glassware. The previously described H-shaped vessels with P4 frit were used as reactors in all solvent-mediated processes[1] Unless stated otherwise, all the solvents were dried over P_2O_5 prior to use. We want to stress, that it may happen that the time of pumping of the samples under high vacuum given here may vary depending on the vacuum achieved in the vacuum line, which is difficult to control in the region below 10^{-3} mbar, especially when the sensor is exposed to various chemicals present in the line. Therefore we suggest to treat these values only as suggestion.

1.1.1. $Li[Al(OR^F)_4]$ from $LiAlH_4$ – improved protocol

A vital improvement of synthesis of $Li[Al(OR^F)_4]$ includes a reaction between excess (1.5 times) of $LiAlH_4$ and $(CF_3)_3COH$ performed in **perfluorohexane** directly in the extractor. Such synthesis, which can be conducted in the apparatus presented in Fig. S1, results in pure product obtained in single step, and ensures economical use of expensive $(CF_3)_3COH$.

The following reagents have been successfully used: $LiAlH_4$ – both Sigma-Aldrich 95% (grey) and Alfa Aesar 97% (almost white) work, but the latter is recommended; $(CF_3)_3COH$ – Fluorochem; perfluorohexane – mostly branched, Fluorochem – a mixture of isomers.

The method does not require purification of substrates, since **i)** perfluorocarbons dissolve only traces of water (in order of ppm)[S2] **ii)** $(CF_3)_3COH$ is dried with excessive $LiAlH_4$ on the frit **iii)** if any hydrated Li compounds were formed, as ionic compounds, they would not dissolve in C_6F_{14} and would remain on the frit; Li[**An**] is the only product which is soluble in perfluorocarbons ($[LiOC(CF_3)_3]_4$ has not been detected in our tests). Another advantage of the method is that an excess[i] of the (inexpensive) alanate can be used resulting in virtually complete consumption of the alcohol. The oxygen dissolved in C_6F_{14} does not distract the reaction when this solvent is used in small amount, which can be achieved when the alcohol is added dropwise (!). Generally, it is recommended to introduce only as much of perfluorocarbon as needed to soak the $LiAlH_4$ left on the frit and keep some of it circulating in the system. In our tests, we were able to obtain as much as 80 g of $Li[Al(OR^F)_4]$ using only 10 ml of C_6F_{14}, although this requires very slow addition of the alcohol. Large portion of $(CF_3)_3COH$ may result in very vigorous reaction and rapid formation of considerable amount of $Li[Al(OR^F)_4]$ on the frit which may hamper the circulation of perfluorohexane. We have also observed, that some samples of $LiAlH_4$ (grey from Sigma-Aldrich) started to react with the alcohol only after induction period of several minutes, probably due to surface inactivation. In such case, if a large portion of the alcohol is added, the reaction may become very vigorous upon initiation and the whole reaction mixture may get hot posing danger (note instability of $LiAlH_4$ above 120°C).

[i] Our experience shows that some vendors supply $LiAlH_4$ which is very contaminated. One of the batches (we do not name the vendor) yielded only <1 g of pure $LiAlH_4$ in extraction from the 25 g of crude chemical with the reported assay of 95% (!). Therefore the method relies on the quality of the starting alanate. Our recommendation is to use >97% purity and at least 1.5 molar excess of $LiAlH_4$ to minimize loses of the alcohol.

The temperature of the hot bath should be *ca.* 70–80°C to boil C_6F_{14} off. To obtain higher yields, it is vital to use an efficient condenser keeping the alcohol in the system, similarly to the previously reported protocols.[S1] The **typical yield** with a highly efficient condenser kept at 0°C (temperature of the condenser and not the oil in the circulation cryostat) is **>97%**, as based on the amount of the alcohol used and the weight of recovered product.

Upon complete removal of perfluorohexane (under dynamic vacuum, 30 minutes at 10^{-2} mbar for a flask kept in still warm bath used during the synthesis) the product is obtained in the form of large grains, and ready to use without further purification, according to FTIR, NMR and XRDP results.

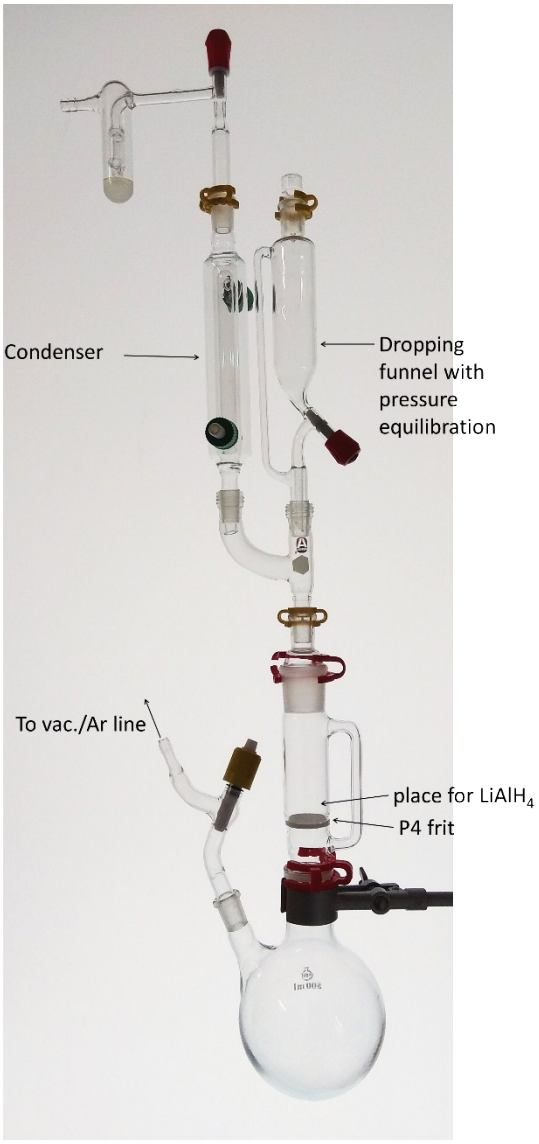

Figure S1. The experimental setup for one-pot synthesis of Li[**An**].

1.1.2. $Li[Al(OR^F)_4]$ from $LiAlH_4$ – previous optimized protocol [S3]

The synthesis uses purified and very finely ground $LiAlH_4$ (=> Dissolution of crude $LiAlH_4$ in Et_2O, filtration and removal of the solvent of the filtrate to constant weight at 100 °C. Care has to be taken, as $LiAlH_4$ decomposes above 120 °C. Thus, a water bath is to be recommended for heating, as this prevents temperatures to get higher than 100 °C.). This purified and very finely ground $LiAlH_4$ is placed in a two-necked Schlenk flask and suspended in petroleum ether (boiling fraction 80 to 100 °C; *ca.* 50

mL per 1 g of $LiAlH_4$). The reaction is routinely done in 100 g product scale with isolated yields around 99 %. One neck is used to connect a pressure-equalizing dropping funnel, while the second is to attach an intensive gas cooler set to −25°C by an external thermostat) with a bubbler at its top. It is extremely important to use the gas cooler instead of a conventional reflux condenser and to cool the gas cooler to low temperature as the evolving H_2 evaporates the very volatile $(CF_3)_3COH$ and one loses yield, if not sticking to this protocol. In addition, the product then contains unreacted $LiAlH_4$, which is detrimental to follow-up chemistry. Thus, 4.1 equivalents of $(CF_3)_3COH$ are added dropwise to the stirred suspension. After all alcohol is consumed, the mixture is heated under reflux for about 3 h. After that time, the Schlenk vessel is cooled down to −25°C to allow complete precipitation of the product. The solvent is decanted off and its remnants are removed under dynamic vacuum (10^{-3} mbar) until constant weight of the sample. This material is completely colorless and may be used directly without further purification. A simple test, if unreacted $LiAlH_4$ is present, is to add a small quantity of the $Li[Al(OR^F)_4]$ to water. If there is no humming sound at all and if it is a clear solution it is clean. If some humming (reaction of $LiAlH_4$ with water) is present or the solution is turbid, one should grind the $Li[Al(OR^F)_4]$ inside a glovebox, suspend it again with petroleum ether and reflux it with addition of extra alcohol similar to the procedure described above. However, with the process described above this is typically not necessary.

1.1.3. $M[Al(OR^F)_4]$, M = Na, K, from $MAlH_4$

The suspension of $MAlH_4$ ($NaAlH_4$ – Sigma-Aldrich, purified by extraction by THF, filtration and evaporation of the solvent, $KAlH_4$ – prepared from KH and $LiAlH_4$ in diglyme/THF[S4,S5]) in hexane was cooled to 0 °C and $(CF_3)_3COH$ (Fluorochem) was slowly added with an excess (*ca.* 150%). The reaction mixture was refluxed for several hours. The solvent has been evaporated and the white solid product has been extracted in Soxhlet extractor using dichloromethane (Sigma-Aldrich, dried over P_2O_5) for M=Na and K, which yield pure products as evaluated by FTIR, NMR and XRDP analyses. Typical yield: >80%.

1.1.4. Ultrasound-induced synthesis of $M[Al(OR^F)_4]$, M = K – Cs, NH_4, N_2H_5

$Li[Al(OR^F)_4]$ and an excess (200%) of ground anhydrous MCl were placed in a reactor together with anhydrous CH_2Cl_2 (*ca.* 5 ml per 1 g of the expected product) and sonicated overnight using a Bandelin DL 156 BH ultrasonic bath with 60% of the maximum output power to reduce heating and loss of water in the bath during the long process. The products were extracted with dichloromethane. Typical yield of the recovered products: M = K *ca.* 40%, Rb *ca.* 65%, Cs *ca.* 85%. Tests with KBr and KF have shown that these halides give much lower yields (30% and 25% respectively). However, with CsF it was already above 80%.

This method is not recommended for the synthesis of Na[**An**] due to very slow reaction and low conversion rate.

1.1.5. Mechanochemical synthesis of $M[Al(OR^F)_4]$, M = K, Rb, Cs, NH_4

$Li[Al(OR^F)_4]$ and an excess of MCl (*ca.* 200%) were mixed and milled for 30 min in 5 min cycles at 1400 rpm using a stainless steel vessel containing a stainless steel milling disc and a LMW-S laboratory vibrating mill (Testchem), Figure S2. Between the milling cycles the vessel was cooled with liquid

nitrogen to maintain room temperature. The product was then extracted using anhydrous dichloromethane. Typical yield: >80%.

A similar procedure has been applied initially for synthesis of $NH_4[Al(OR^F)_4]$, however, it resulted in the product contaminated by $[N_2H_7][Al(OR^F)_4]$, probably due to a significant excess of NH_4Cl.

While this is a very convenient and fast method, the samples prepared this way may be slightly contaminated with small amount of metal halides which may be transferred through the glass frit due to very small grain size.

Figure S2. The LMW-S vibrational mill (left) and a stainless steel disc bowls (right) used for mechanochemical synthesis.

1.1.6. Synthesis of $Ag[Al(OR^F)_4]$

The synthesis starts from purified $Li[Al(OR^F)_4]$ and *ca.* 40% molar excess of AgF (Fluorochem – we have found the compound of very good quality and used it with success despite previous suggestions to use another vendor of the chemical). The excess of AgF can be also at the level of 15-20%, but since AgF can be in the state of fine powder mixed with larger chunks, to provide its higher surface area we recommend the higher value. For each gram of $Li[Al(OR^F)_4]$ we recommend at least 2 ml of SO_2, what facilitates extraction of $Ag[Al(OR^F)_4]$. The reaction mixture is left on vigorous stirring. Complete conversion is achieved after 7-10 days. The typical yield of isolated product is *ca.* 85%, i.e. similar for the route with perfluorohexane used as reaction medium.[S6]

1.1.7. $M[Al(OR^F)_4]$, M = NO

The compound was synthesized according to the previously reported method.[S7]

1.1.8. Ag[***alfal***] and Cu[***alfal***]

The silver salt was obtained according to literature protocol[S8] and was crystallized from C_6F_6 (though the compound is also soluble in C_6F_{14}).

Route to crystals of Cu[***alfal***] is described in the main manuscript. Note, that heating to *ca.* 45°C of dry $Cu[Al(OR^F)_4]$ leads to amorphous solid. Slight contamination with Ag visible in the crystal structure is the result of presence of silver salt (most probably AgI, but presence of minor amounts of $Ag[Al(OR^F)_4]$ cannot be overruled) during heating of $Cu[Al(OR^F)_4]$.

1.2. Analytical procedures

1.2.1. FTIR spectroscopy

The FTIR spectra of the solid samples were measured either in transmission or in reflection geometry. For the measurements in transmission mode a Vertex 80v FTIR spectrometer (Bruker) has been used. The samples were placed between the windows made of AgCl. The measurements in reflection geometry were conducted using Nicolet Magna-IR spectrometer with a Diamond-ATR module with ATR corrections applied.

1.2.2. Raman spectroscopy

Raman spectra have been recorded on a Bruker VERTEX 70 spectrometer with RAM II module at 1064 nm (Nd-YAG laser). Samples were closed in a flame-sealed glass capillaries.

1.2.3. Powder X-ray diffraction

Powder X-ray diffraction (XRDP) patterns of the samples sealed inside quartz capillaries (diameter of 0.5–1 mm) were measured on three diffractometers: Bruker D8 Discover diffractometer (parallel beam; the $CuK_{\alpha1}$ and $CuK_{\alpha2}$ radiation), Panalytical X'Pert Pro diffractometer (parallel beam; the $CoK_{\alpha1}$ and $CoK_{\alpha2}$ radiation) and Stoe Stadi P powder diffractometer using monochromated Mo $K_{\alpha1}$ radiation and PSD or Mythen 1K microstrip X-ray detector. They are marked according to the radiation used.

1.2.4. Single crystal diffraction

The single crystals suitable for structure determination of $M[Al(OR^F)_4]$ were grown in various ways. Good quality crystals of the salts containing larger cations, M = K, Rb, NH_4, N_2H_5, were easily obtained from the saturated solutions in dichloromethane. For M=Na a prolonged (days) crystallization from slowly cooled (from 25°C down to −40°C in *ca.* 24 h) FC-770 solution was required to obtain crystals of sufficient quality. During the measurements the crystals were immersed in the protective perfluorinated oil (Krytox 1531).

Data collection and reduction was performed with one of the two setups: Agilent Supernova X-ray diffractometer with Kα-Cu radiation (microsource) with data reduction performed by CrysAlisPro software (v. 38.43)[S9] or Bruker Smart Apex II Quazar single crystal diffractometer, graphite-monochromated Mo-Kα radiation from microsource, data collection and reduction: APEX v2013.10-0 and SAINT V8.34A; absorption correction: TWINABS 2012/1. Structure solution: SHELXT[S10], refinement against F^2 in Shelxl-2013,[S10] with ShelXle as GUI software.[S11] The disorder of the $–OC(CF_3)_3$ groups was resolved using DSR.[S12] Graphical presentation of crystal structures has been performed with Vesta.[S13]

1.2.5. TGA/DSC

Thermal decomposition was investigated using a combined thermogravimeter (TGA) and differential scanning calorimeter (DSC) from Netzsch – STA 409 PG. The samples were placed inside Al_2O_3 crucibles, and were heated at $5^oC\ min^{-1}$ rate under a constant Ar (99.9999%) flow. The evolved gases were analyzed with a quadrupole mass spectrometer (MS) QMS 403 C (Pfeiffer Vacuum), connected to the TGA/DSC device by a quartz capillary preheated to 200°C to avoid condensation of low-boiling volatiles. Range of M/Z from 1 to at least 120 was studied.

1.2.6. NMR spectra

NMR spectra were recorded on Bruker AVANCE III HD 300 MHz or 500 MHz. Samples highly susceptible to traces of water (Li, Na, N-compounds, Cl_3CCN solvates) were placed in 4mm air-tight NMR tubes equipped with PTFE valve and dissolved in SO_2. Deuterated solvents (acetone, $CDCl_3$ or CD_2Cl_2) for these compounds were placed in outer, 5mm tube. K-Cs salts were dissolved in CD_2Cl_2 (not dried) in air.

It was observed, that in every ^{19}F measurement there is a weak signal ca. 0.8 ppm less negative the main one. This is the signal from the free $HOC(CF_3)_3$, which is commonly found in the spectra of $[Al(ORF)_4]^-$ salts. For ^1H spectra, the signals from NH_4 and N_2H_5 are not very strong as compared to impurities present in deuterated $(CD_3)_2CO$ (H_2O and not perdeuterated acetone).

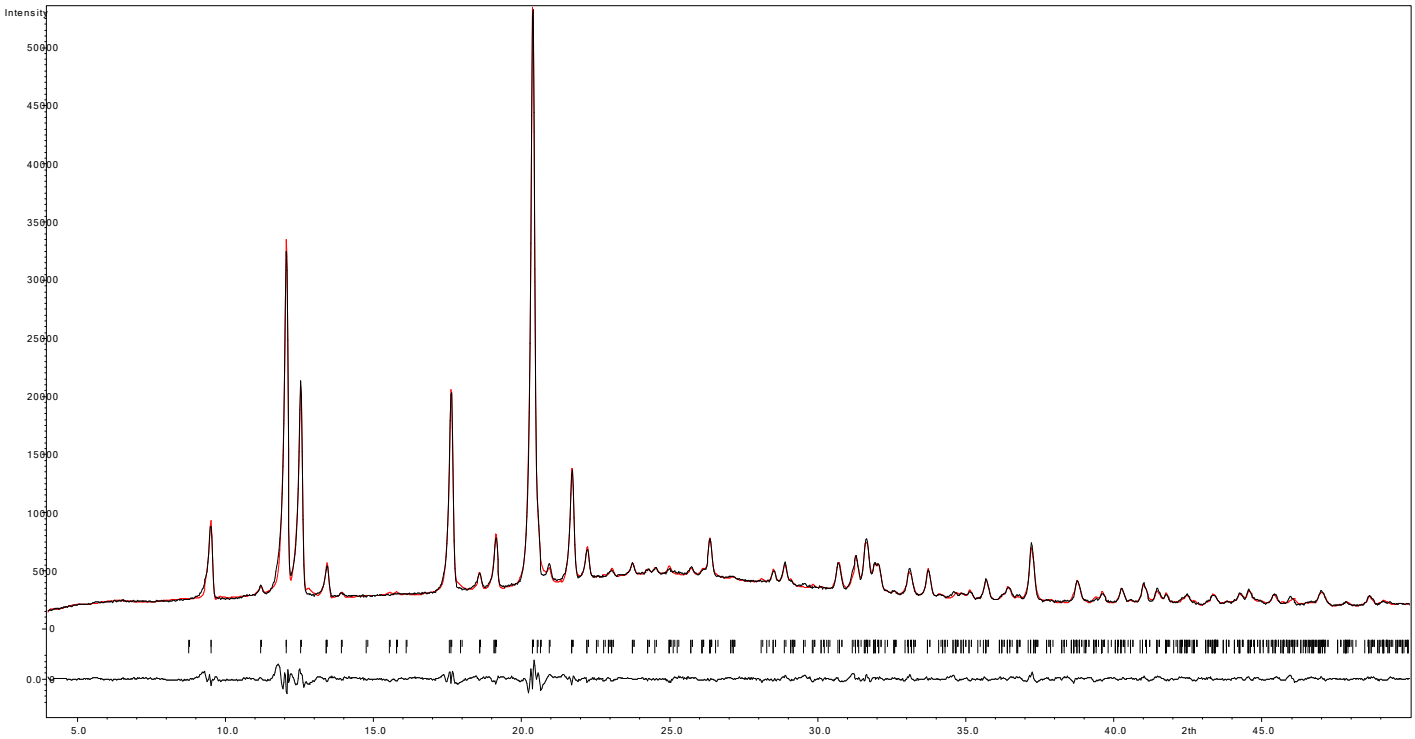

2. Supplementary analytical results

Figure S3. The Rietveld fit for the sample of $Li[Al(OR^F)_4]$ prepared according to the procedure described in the section 1.1.1. The measured powder pattern (black line), the calculated powder pattern (red line), the Bragg reflections and the difference plot (bottom) have been shown. wRp = 3.95%, T = *ca.* 295 K, a = 10.104(4) Å, b = 13.886(6) Å, c = 21.504(8) Å, V = 3017(2) $Å^3$ (*ca.* 6.8% expansion as compared to 100 K). Co Kα.

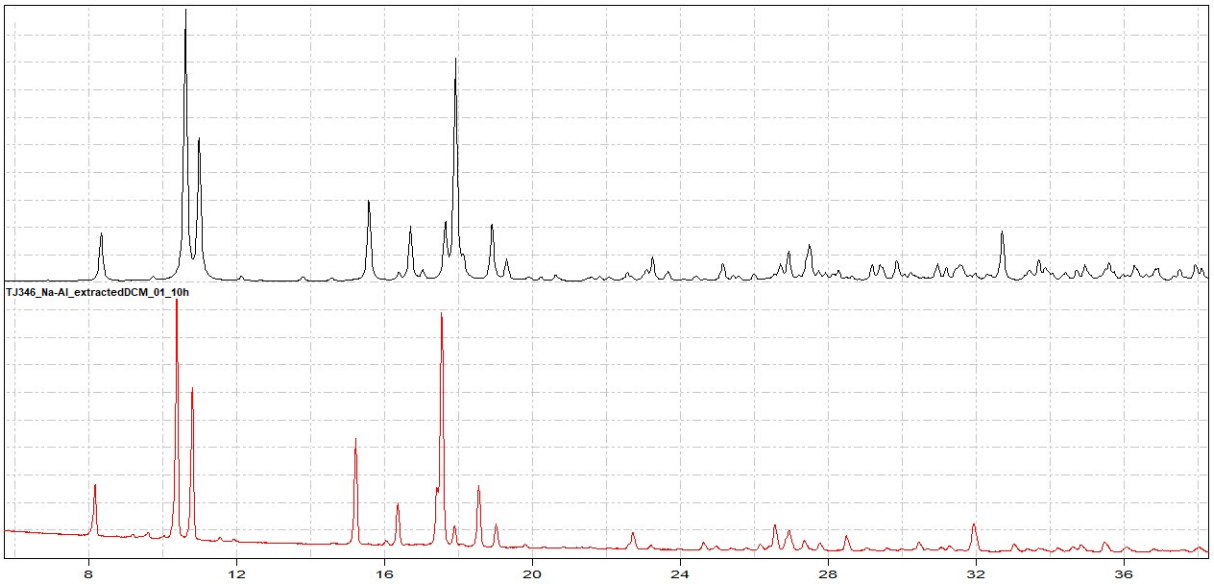

Figure S4. XRDP patterns of $Na[Al(OR^F)_4]$: experimental (RT, bottom – red curve; **prepared as described in 1.1.3**) and generated from the crystal structure (data for 100 K, top – black curve). The shift in positions of reflexes and differences in intensities are the result of different measurement temperatures. Cu Kα.

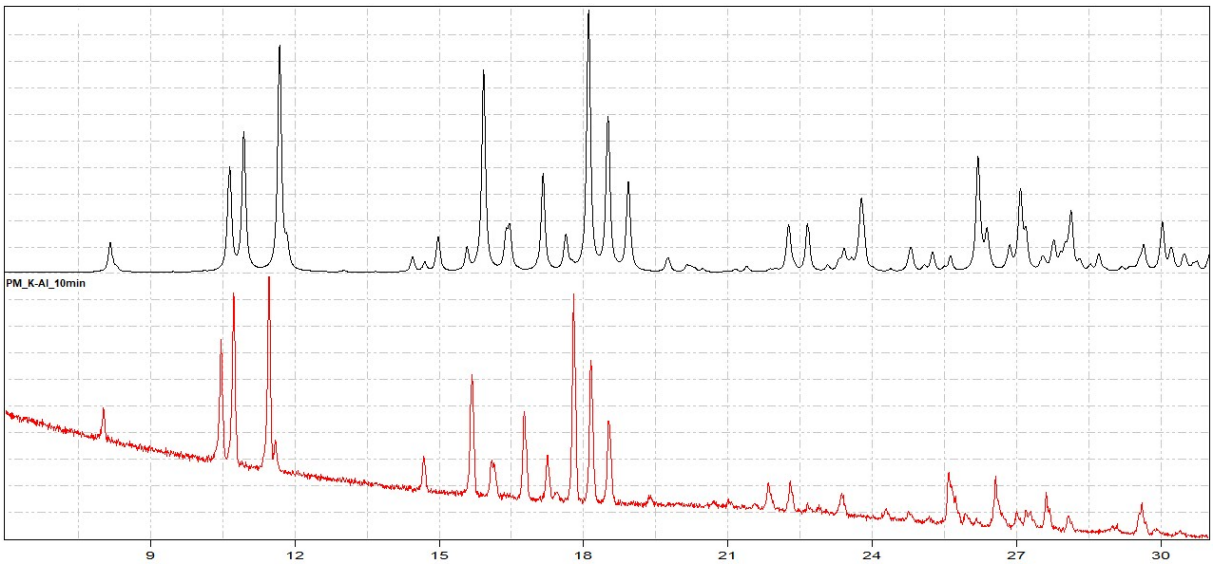

Figure S5. XRDP patterns of $K[Al(OR^F)_4]$: experimental (RT, bottom – red curve; **prepared as described in 1.1.4**) and generated from the crystal structure (data for 100 K, top – black curve). The shift in positions of reflexes and differences in intensities are the result of different measurement temperatures. Cu Kα.

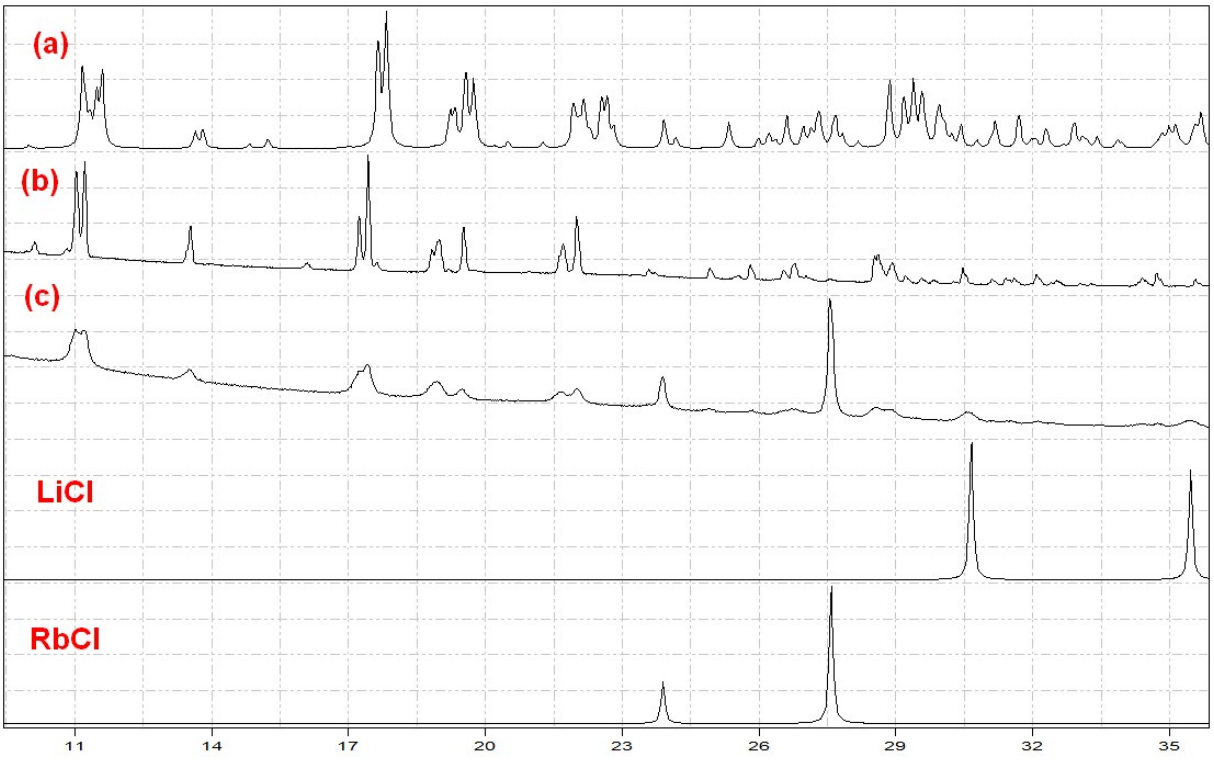

Figure S6. XRDP patterns of $Rb[Al(OR^F)_4]$: (a) generated from the crystal structure (data for 100 K); (b) experimental (RT, **prepared as described in 1.1.5 – extracted with dichloromethane and precipitated with hexane**[ii]); (c) experimental (RT, **prepared as described in 1.1.5 – before extraction**). The patterns generated for LiCl and RbCl were included for comparison. The shift in positions of reflexes and differences in intensities are the result of different measurement temperatures. Cu Kα.

[ii] Precipitation with hexane instead of evaporation has been applied as $Li[Al(OR^F)_4]$ of low purity was used in this particular synthesis.

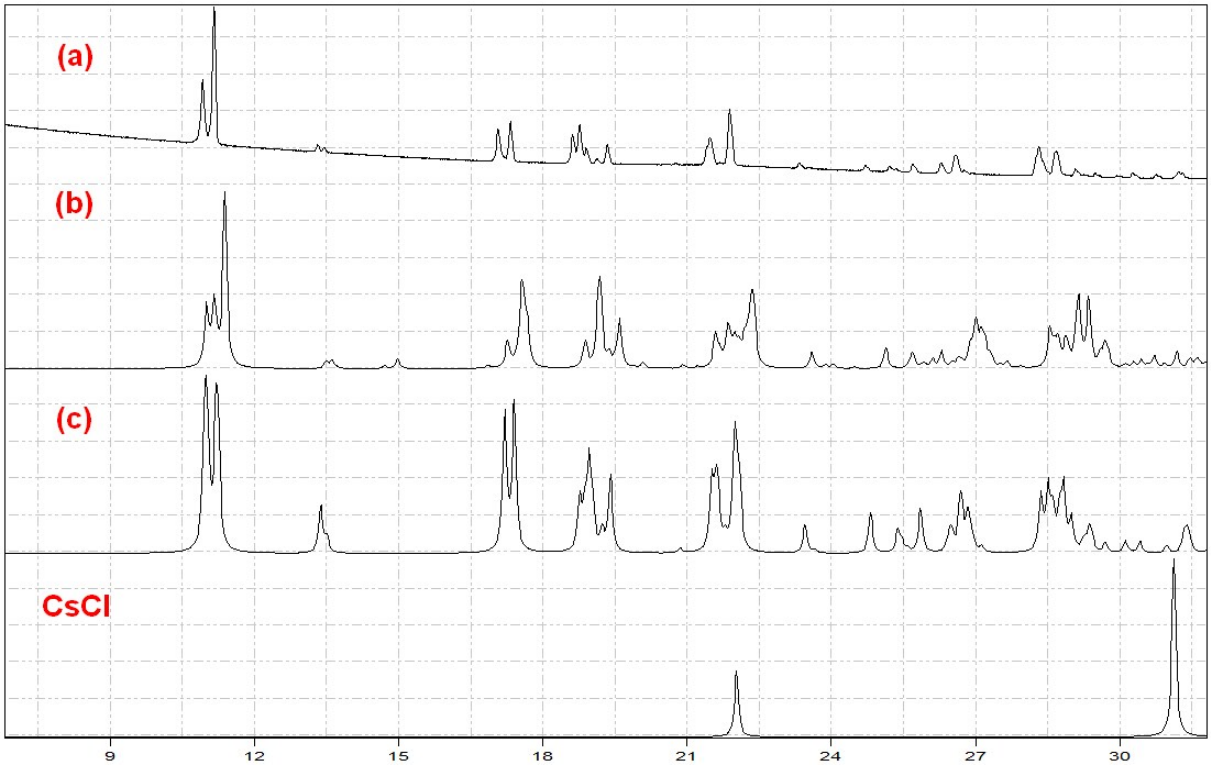

Figure S7. XRDP patterns of $Cs[Al(OR^F)_4]$: (a) experimental (RT), **prepared as described in 1.1.5 – extracted with dichloromethane and precipitated with hexane**[iii]); (b) generated from the ***P*1** crystal structure (data for 100 K); generated from the ***Cc*** crystal structure (data for 223 K).[S14] The pattern generated for CsCl was also included for comparison. The shift in positions of reflexes and differences in intensities are the result of different measurement temperatures. Cu Kα.

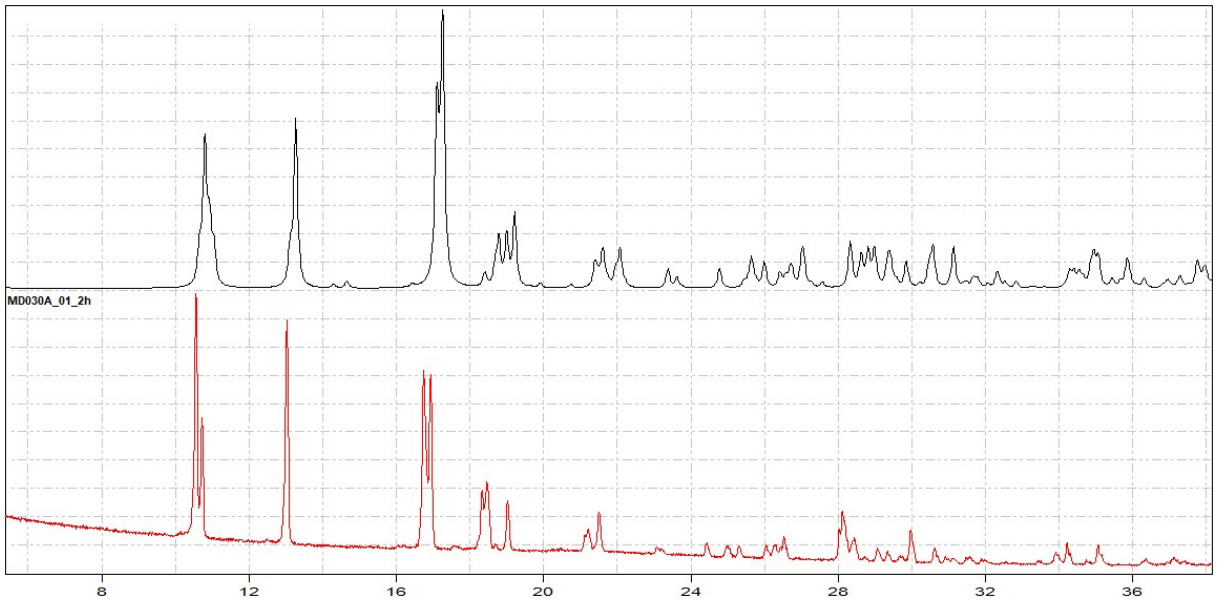

Figure S8. XRDP patterns of $NH_4[Al(OR^F)_4]$: top – generated from the crystal structure (data for 100 K); bottom – experimental (RT), the sample **prepared as described in 1.1.4, extracted with dichloromethane**. The shift in positions of reflexes and differences in intensities are the result of different measurement temperatures – possibly a polymorphic transition occurs. Cu Kα.

[iii] Precipitation with hexane instead of evaporation has been applied as $Li[Al(OR^F)_4]$ of low purity was used in this particular synthesis.

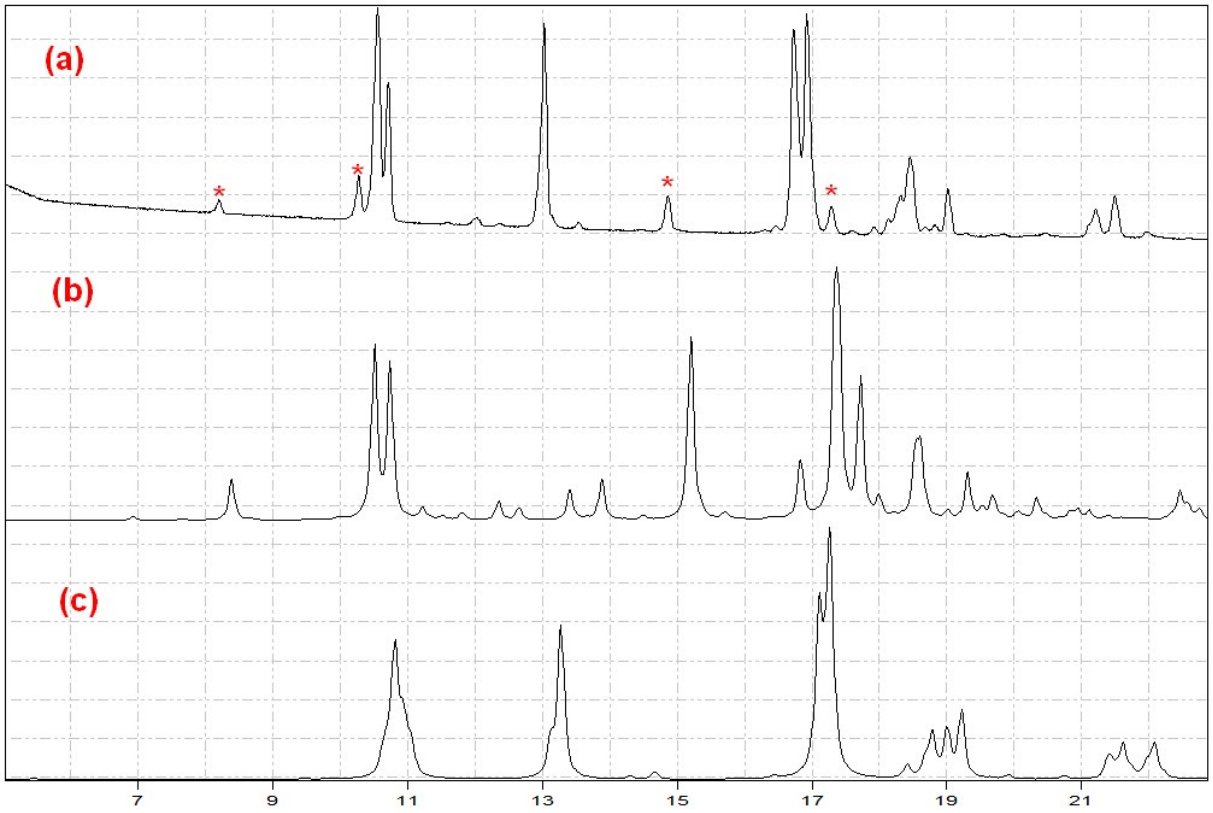

Figure S9. XRDP patterns of: (a) the sample of $NH_4[Al(OR^F)_4]$ **prepared as described in 1.1.5 – extracted with dichloromethane**, the characteristic peaks from $N_2H_7[Al(OR^F)_4]$ have been marked with an asterisk; (b) generated from the crystal structure of $N_2H_7[Al(OR^F)_4]$ (data for 100 K); (c) generated from the crystal structure of $NH_4[Al(OR^F)_4]$ (data for 100 K). The shift in positions of reflexes and differences in intensities are the result of different measurement temperatures – possibly a polymorphic transition occurs for $NH_4[Al(OR^F)_4]$. Cu Kα.

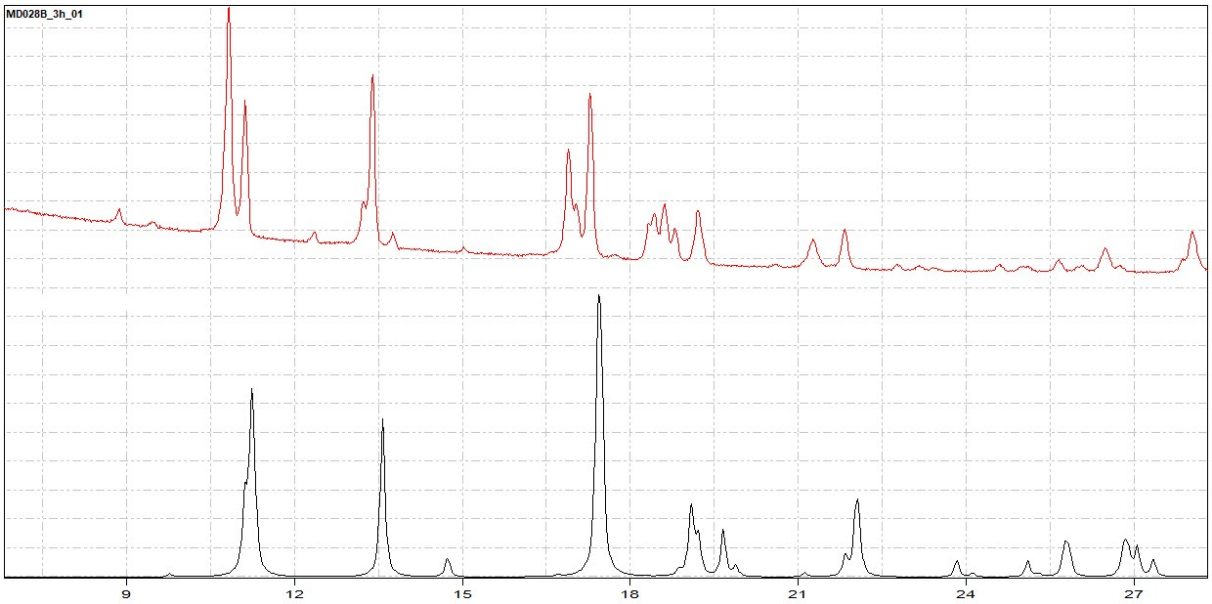

Figure S10. XRDP patterns of: the sample of $N_2H_5[Al(OR^F)_4]$ **prepared as described in 1.1.4 – extracted with dichloromethane** (top); generated from the crystal structure of $N_2H_5[Al(OR^F)_4]$ (data for 100 K). The shift in positions of reflexes and differences in intensities are the result of different measurement temperatures – possibly a polymorphic transition occurs. Cu Kα.

Table S1. The absorption bands observed in the FTIR spectra of $M[Al(OC(CF_3)_3)_4]$ salts, [cm^{-1}]. The values reported for tetraalkylammonium salts (TAA), i.e. [Me_4N], [Et_4N] and [Bu_4N], are listed for comparison . vw – very weak, w – weak, m – medium, s – strong, vs – very strong, sh – shoulder, br – broad, R – Raman active mode for the anions of higher symmetry.

Li	Na	Ag	K	Rb	Cs	NH_4 *	N_2H_5 *	NO	TAA [S15]
456 vw	455 vw	439 vw	447 vw	448 w	447 w	448 s	448 s, sh	447 vw	446–449
481 vw	480 vw	468 vw	-	-		-	-	-	
538 vw	538 vw	537 vw	535 w	536 w	537 w	537 m	536 w	535 vw	536–538
550 vw	550 vw	554 vw	-	-		-	-	-	
565 vw	565 vw	568 vw	562 vw	561 w	561 vw	562 m	560 w	560 vw	559–562
572 vw	573 vw	578 vw	573 vw	572 vw	572 vw	571 w	572 vw	573 vw	571–573
581 vw	581 vw		-	-		-		-	
726 m	726 m	728 m	726 s	726 m	727 s	727 vs	727 s	726 s	726–727
729 m	729 sh	-	-	-		-		-	
745 vw	745 vw	745 vw	-	-		-		-	744–747 R
756 vw	756 vw		757 vw	755 vw	756 vw	756 w	755 w	757 vw	755–756
760 vw	759 vw	760 vw	-	-		-		-	
799 vw	800 vw	800 vw							794–799 R
			-	-				-	
844 vw	844 vw	-	833 vw	834 vw	834 vw	834 w	836 w	832 vw	830–833
864 vw	866 vw	864 vw	-				878 vw	-	
963 sh	961 sh		967 sh	963 s	964 vs	962 vs	971 vs		967 sh
976 s	976 vs	974 s	972 vs	975 m	976 s	975 vs		972 s	973–976
						1022 vw, sh	1021		
							1050 vw		
1108 vw	1115 vw	1129 vw	1122 w	1125w	1130 vw	1120 w	1127 vw, sh	1119 vw	1133–1139 R
-	-	1155 vw	1155 w	-				-	
1175 m	1175 w	1176 vw	1173 m	1185 m	1183 m	1177 w	1183 m, sh	1171 w	1163–1176
1216 s	1216 s	1215 s	1208 vs	1225 vs	1224 vs	1224 vs	1220 vs	1208 vs	1217–1223
1230 sh			1218 sh						
1249 vs	1251 vs	1253 vs	1253 vs	1247 vs	1247 vs	1245 vs	1249 vs	1252 vs	1236–1240
				1265 s	1266 vs	1266 s			
1277 s	1272 vs	1272 vs	1278 vs		1276 vs	1276 s	1273 vs	1279 vs	1271–1274
1302 sh	1301 sh	1302 w	1298 s	1297 m	1306 s	1301 s	1300 s	1298 s	1296–1299
1352 vw	1355 vw	1367 vw	1355 m	1354 w	1357 m	1354 m	1355 m	1354 w	1349–1353
							1517 w		
						1434 m	1540 vw		
							1604 w, br		
							3186 vw		
							3205 w		
						3236 sh, br	3246 w		
						3324 m, br	3300 m		
						3434 sh, br	3327 sh		
							3413 w		

* samples measured on AgCl windows

Raman spectra with the most important bands marked

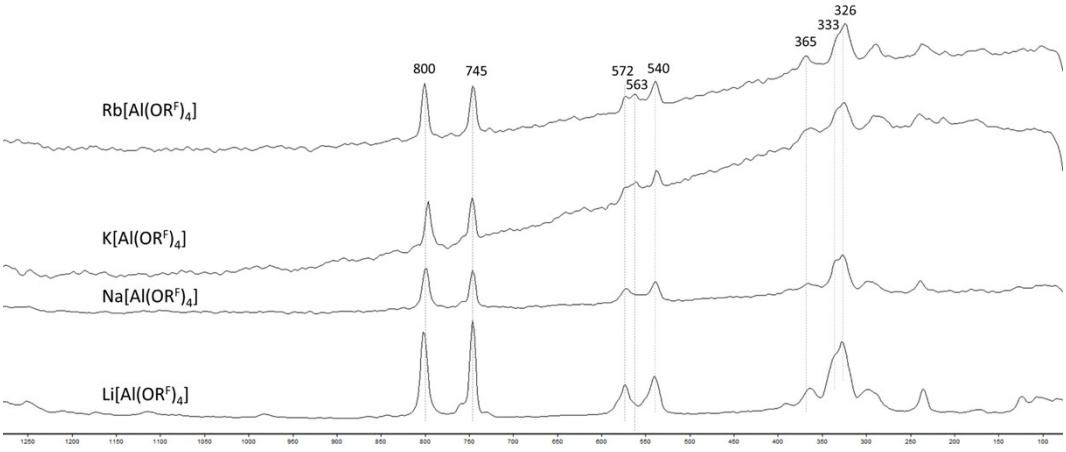

NMR spectra

$NH_4[Al(OR^F)_4]$

19F

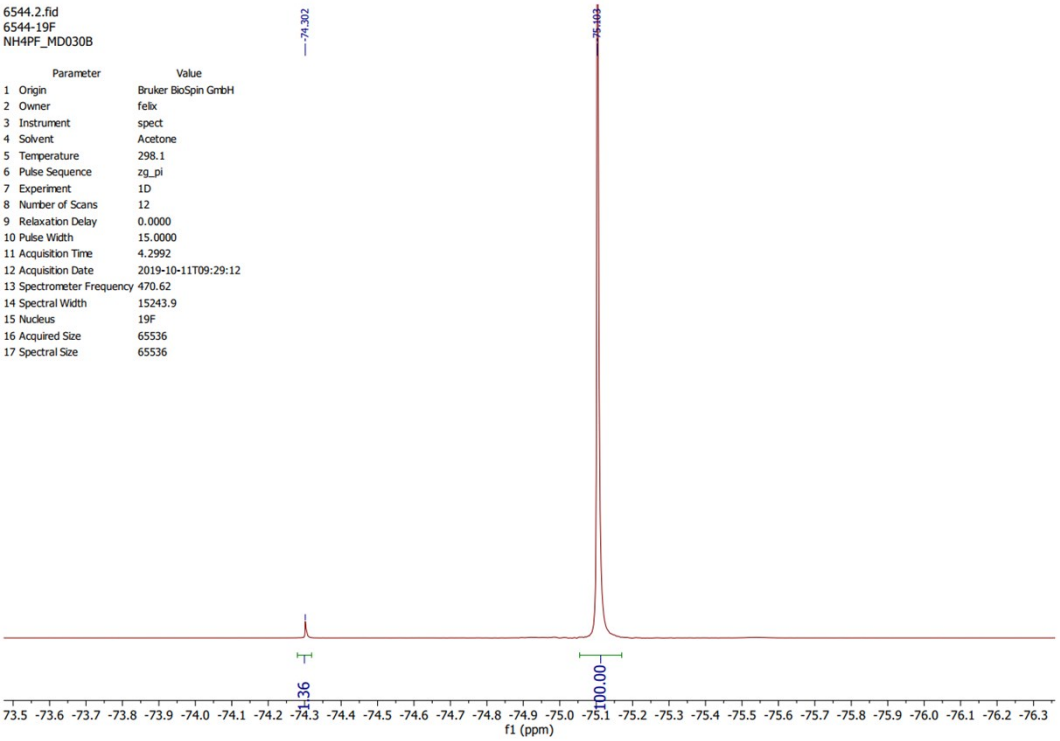

	Parameter	Value
1	Origin	Bruker BioSpin GmbH
2	Owner	felix
3	Instrument	spect
4	Solvent	Acetone
5	Temperature	298.1
6	Pulse Sequence	zg_pi
7	Experiment	1D
8	Number of Scans	12
9	Relaxation Delay	0.0000
10	Pulse Width	15.0000
11	Acquisition Time	4.2992
12	Acquisition Date	2019-10-11T09:29:12
13	Spectrometer Frequency	470.62
14	Spectral Width	15243.9
15	Nucleus	19F
16	Acquired Size	65536
17	Spectral Size	65536

27Al

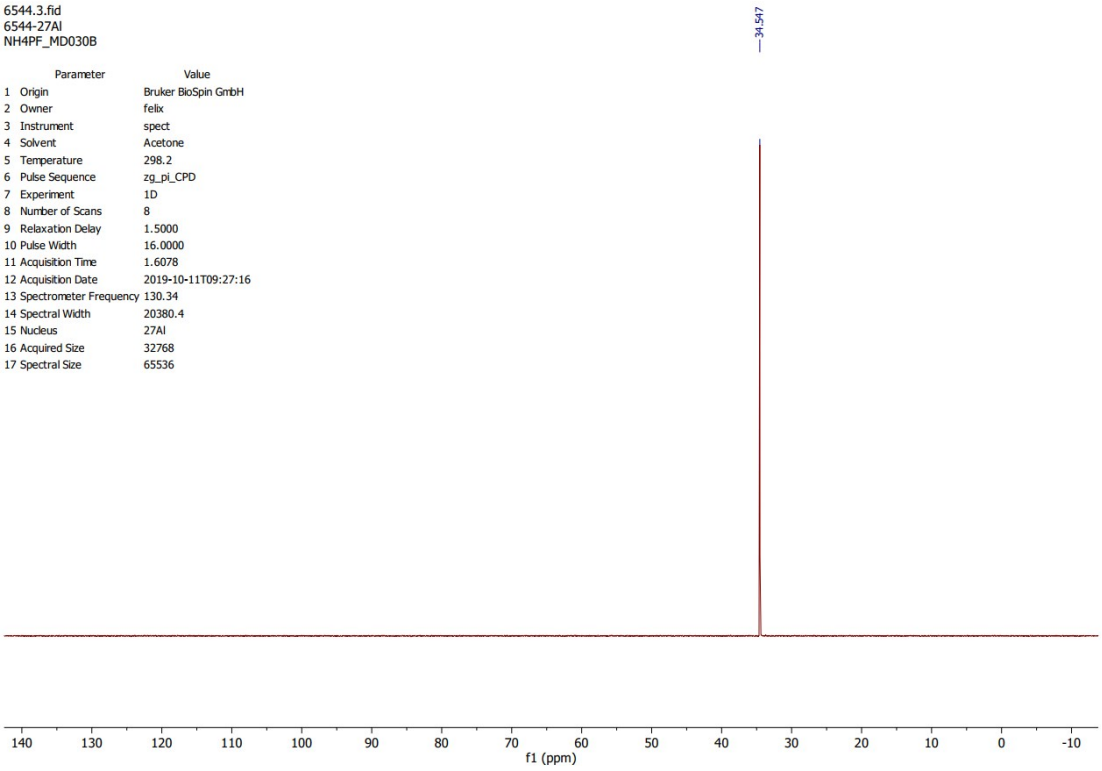

	Parameter	Value
1	Origin	Bruker BioSpin GmbH
2	Owner	felix
3	Instrument	spect
4	Solvent	Acetone
5	Temperature	298.2
6	Pulse Sequence	zg_pi_CPD
7	Experiment	1D
8	Number of Scans	8
9	Relaxation Delay	1.5000
10	Pulse Width	16.0000
11	Acquisition Time	1.6078
12	Acquisition Date	2019-10-11T09:27:16
13	Spectrometer Frequency	130.34
14	Spectral Width	20380.4
15	Nucleus	27Al
16	Acquired Size	32768
17	Spectral Size	65536

1H

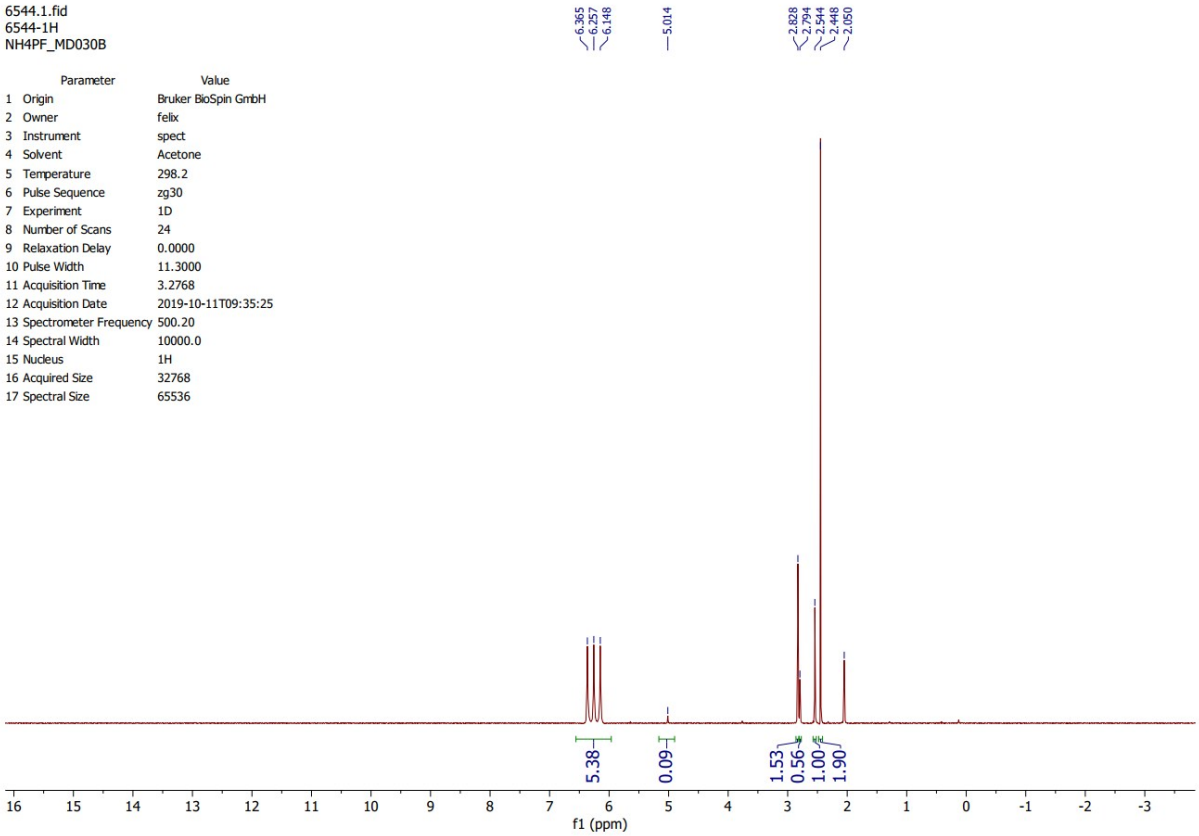

The signals between 2 and 3 ppm come from impurities of $(CD_3)_2CO$. The origin of the weak signal at 5.014 ppm remains unknown.

$N_2H_5[Al(OR^F)_4]$

19F

6545.2.fid
6545-19F
N2H5PF_MD042B

	Parameter	Value
1	Origin	Bruker BioSpin GmbH
2	Owner	felix
3	Instrument	spect
4	Solvent	Acetone
5	Temperature	298.2
6	Pulse Sequence	zg_pi
7	Experiment	1D
8	Number of Scans	8
9	Relaxation Delay	0.0000
10	Pulse Width	15.0000
11	Acquisition Time	4.2992
12	Acquisition Date	2019-10-11T11:17:37
13	Spectrometer Frequency	470.62
14	Spectral Width	15243.9
15	Nucleus	19F
16	Acquired Size	65536
17	Spectral Size	65536

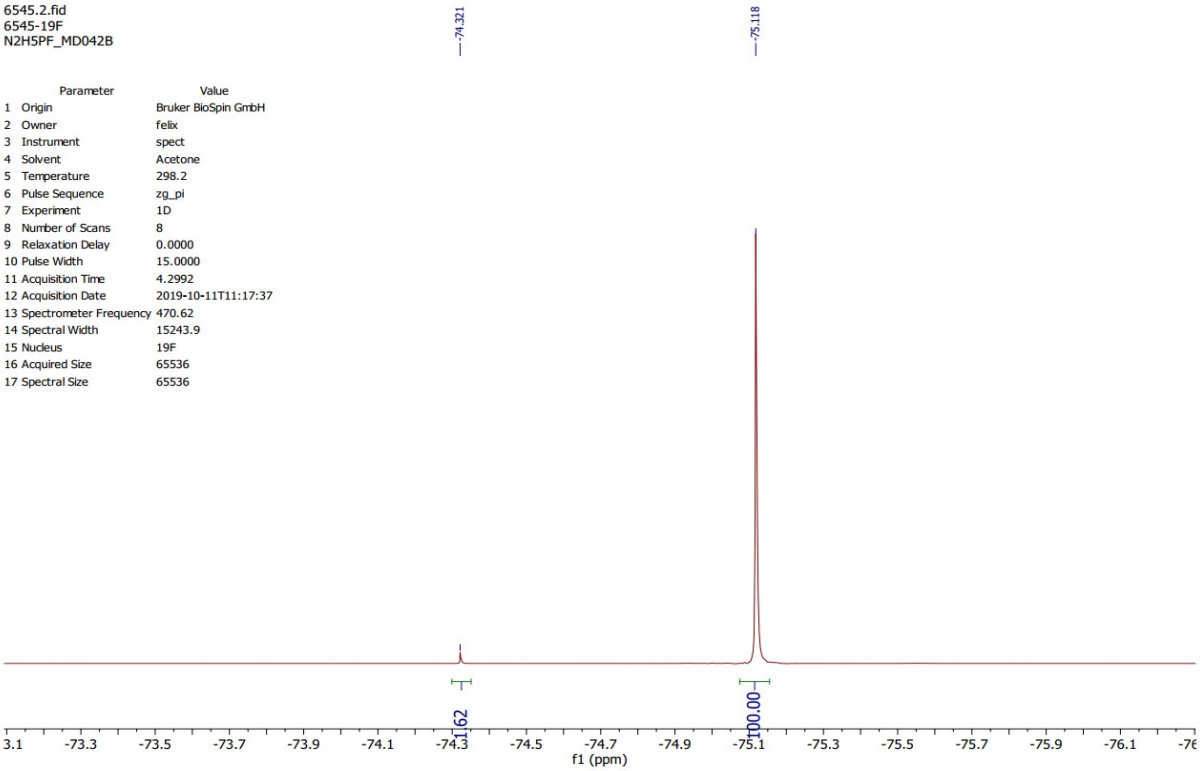

1H

6545.1.fid
6545-1H
N2H5PF_MD042B

	Parameter	Value
1	Origin	Bruker BioSpin GmbH
2	Owner	felix
3	Instrument	spect
4	Solvent	Acetone
5	Temperature	298.1
6	Pulse Sequence	zg30
7	Experiment	1D
8	Number of Scans	16
9	Relaxation Delay	0.0000
10	Pulse Width	11.3000
11	Acquisition Time	3.2768
12	Acquisition Date	2019-10-11T11:15:23
13	Spectrometer Frequency	500.20
14	Spectral Width	10000.0
15	Nucleus	1H
16	Acquired Size	32768
17	Spectral Size	65536

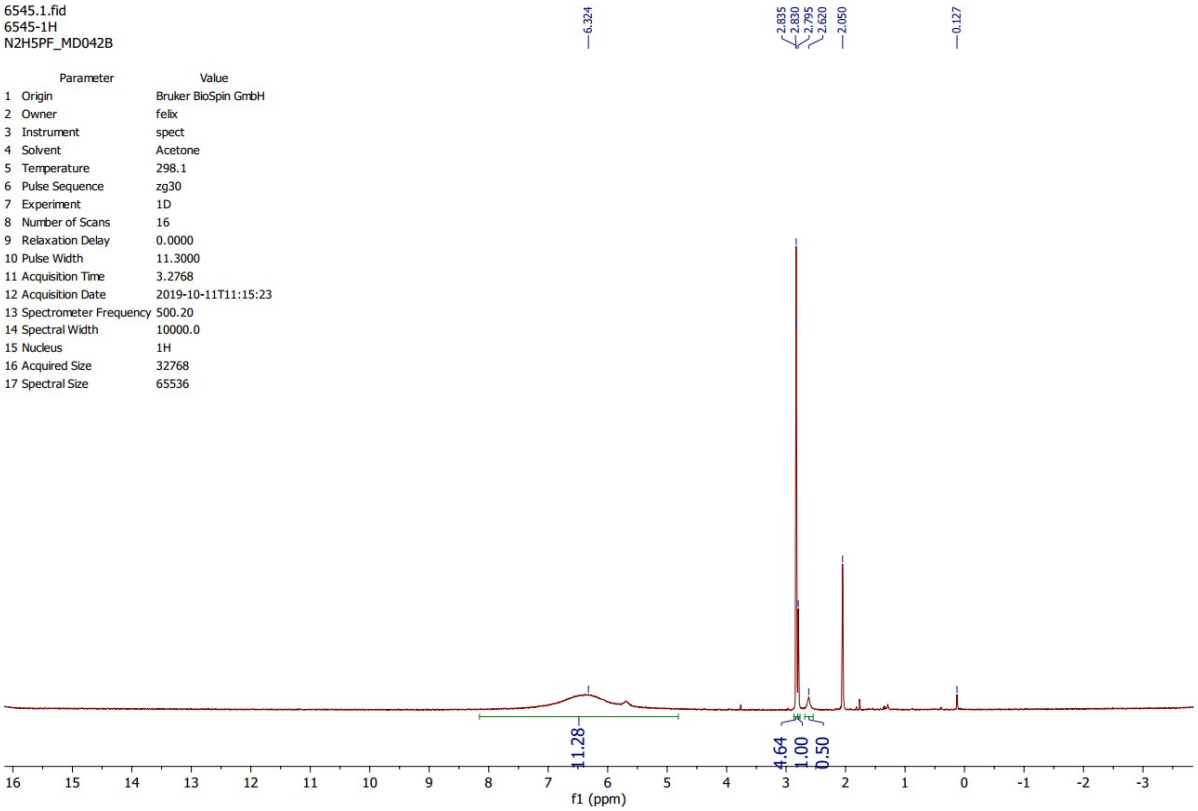

27Al

6545.3.fid
6545-27Al
N2H5PF_MD042B

	Parameter	Value
1	Origin	Bruker BioSpin GmbH
2	Owner	felix
3	Instrument	spect
4	Solvent	Acetone
5	Temperature	298.1
6	Pulse Sequence	zg_pi_CPD
7	Experiment	1D
8	Number of Scans	4
9	Relaxation Delay	1.5000
10	Pulse Width	16.0000
11	Acquisition Time	1.6078
12	Acquisition Date	2019-10-11T11:19:02
13	Spectrometer Frequency	130.34
14	Spectral Width	20380.4
15	Nucleus	27Al
16	Acquired Size	32768
17	Spectral Size	65536

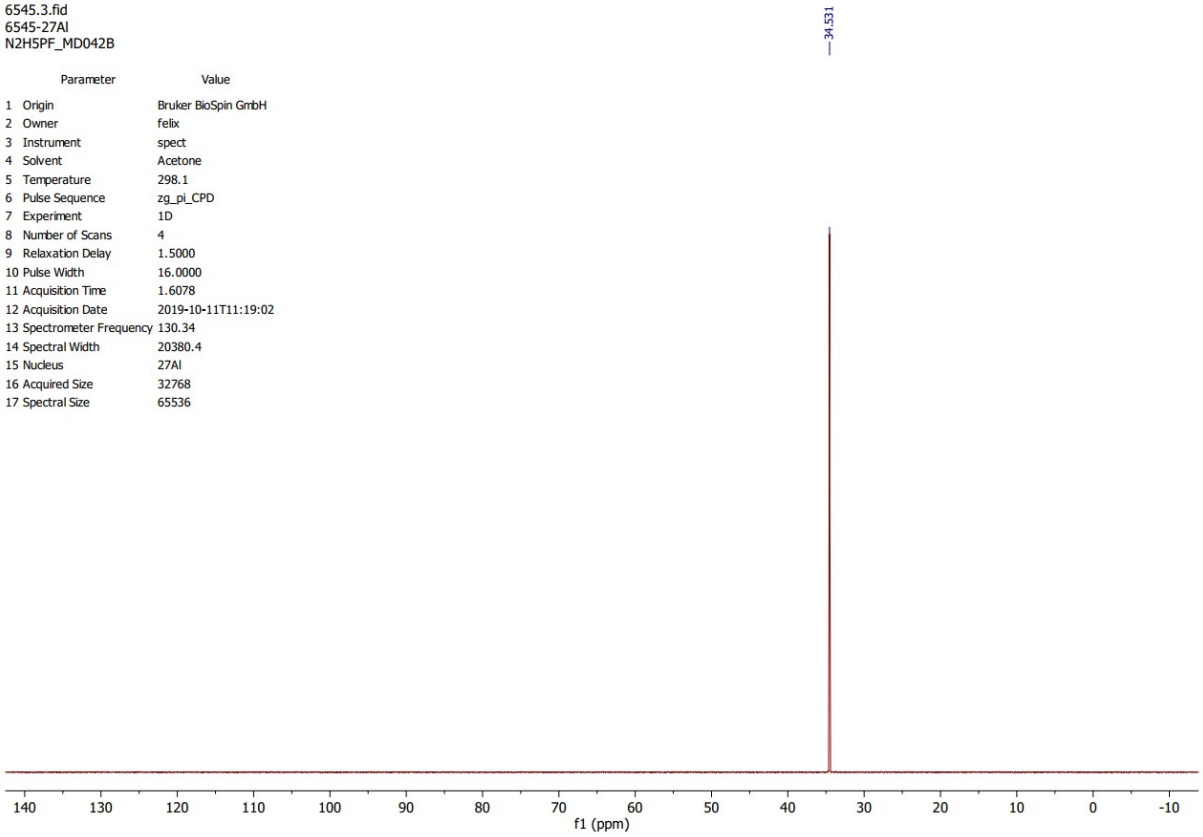

$Li[Al(OR^F)_4]$

19F

	Parameter	Value
1	Comment	23903-19F LiPF_09.2019
2	Origin	Bruker BioSpin GmbH
3	Solvent	CDCl3
4	Temperature	298.1
5	Pulse Sequence	zg_pi
6	Number of Scans	100
7	Receiver Gain	200
8	Relaxation Delay	0.0000
9	Pulse Width	15.0000
10	Acquisition Time	0.9787
11	Acquisition Date	2019-10-10T13:36:15
12	Modification Date	2019-10-10T13:36:16
13	G to G'	1.00000000
14	Echo Delay	0.0000
15	Gradient Duration	0.0000
16	Spectrometer Frequency	282.47
17	Spectral Width	66964.3
18	Lowest Frequency	-61729.2
19	Nucleus	19F
20	Acquired Size	65536
21	Spectral Size	131072

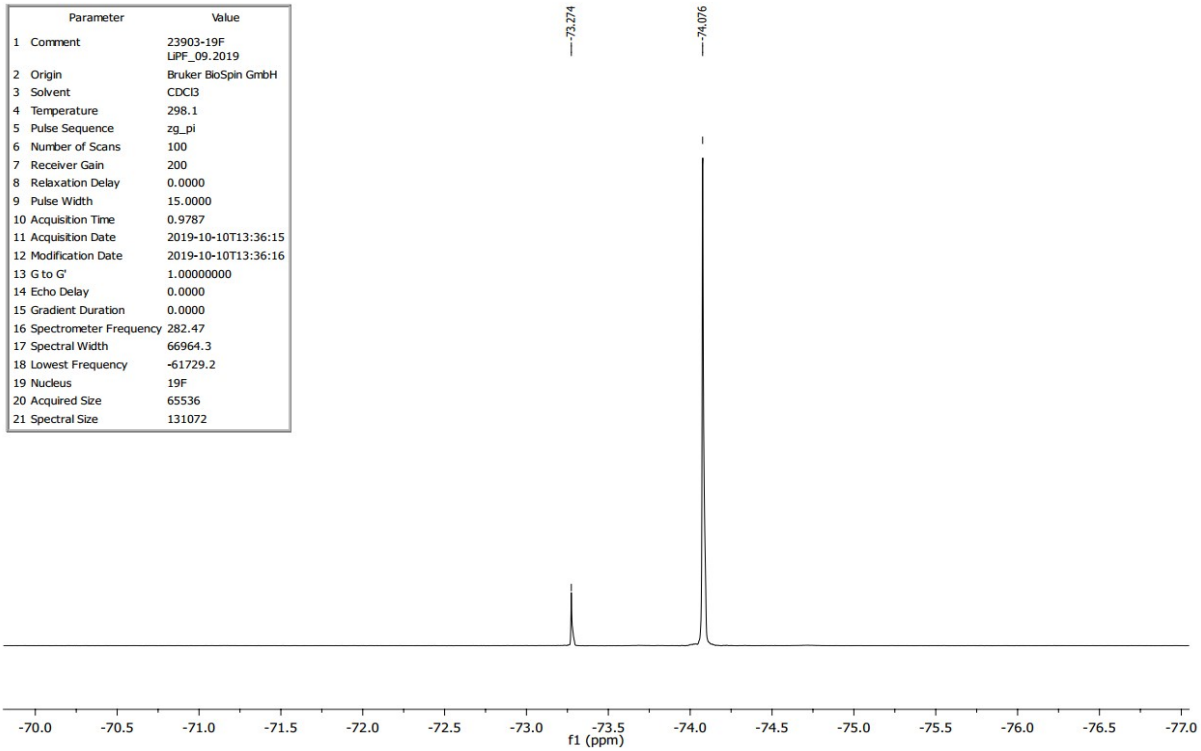

27Al

	Parameter	Value
1	Comment	23903-127Al LiPF_09.2019
2	Origin	Bruker BioSpin GmbH
3	Solvent	CDCl3
4	Temperature	298.2
5	Pulse Sequence	zg_pi_CPD
6	Number of Scans	12
7	Receiver Gain	179
8	Relaxation Delay	1.5000
9	Pulse Width	20.5500
10	Acquisition Time	1.3981
11	Acquisition Date	2019-10-10T14:40:18
12	Modification Date	2019-10-10T14:40:27
13	G to G'	1.00000000
14	Echo Delay	0.0000
15	Gradient Duration	0.0000
16	Spectrometer Frequency	78.22
17	Spectral Width	23437.5
18	Lowest Frequency	-3896.5
19	Nucleus	
20	Acquired Size	32768
21	Spectral Size	65536

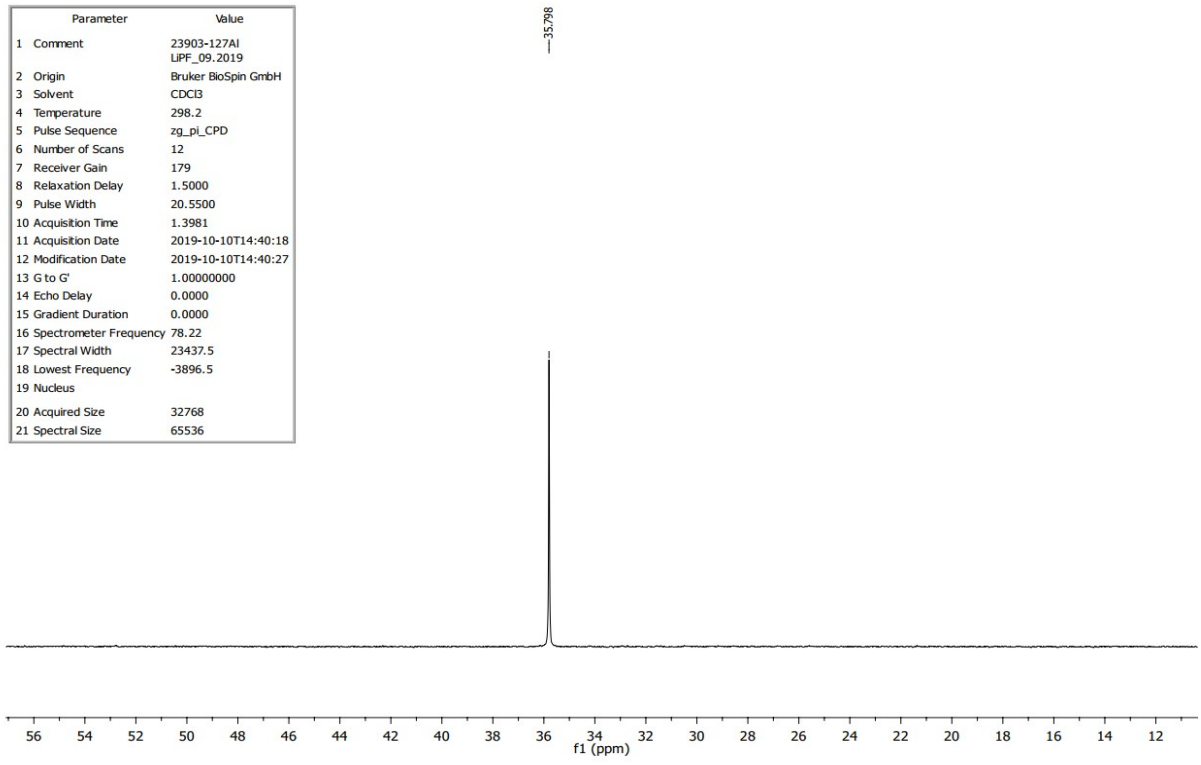

$Na[Al(OR^F)_4]$

19F

	Parameter	Value
1	Comment	23904-19F NaPF
2	Origin	Bruker BioSpin GmbH
3	Solvent	CDCl3
4	Temperature	298.2
5	Pulse Sequence	zg_pi
6	Number of Scans	32
7	Receiver Gain	200
8	Relaxation Delay	0.0000
9	Pulse Width	15.0000
10	Acquisition Time	0.9787
11	Acquisition Date	2019-10-10T13:46:50
12	Modification Date	2019-10-10T13:47:16
13	G to G'	1.00000000
14	Echo Delay	0.0000
15	Gradient Duration	0.0000
16	Spectrometer Frequency	282.47
17	Spectral Width	66964.3
18	Lowest Frequency	-61729.2
19	Nucleus	19F
20	Acquired Size	65536
21	Spectral Size	131072

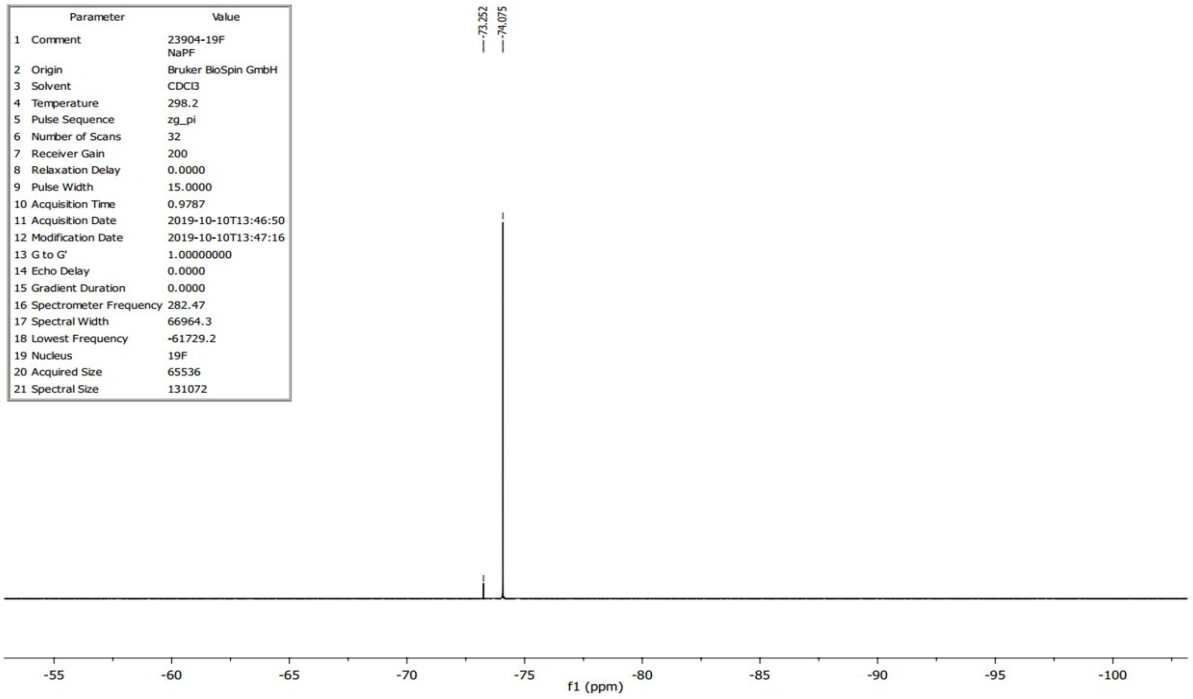

27Al

	Parameter	Value
1	Comment	23904-127Al NaPF
2	Origin	Bruker BioSpin GmbH
3	Solvent	CDCl3
4	Temperature	298.2
5	Pulse Sequence	zg_pi_CPD
6	Number of Scans	24
7	Receiver Gain	200
8	Relaxation Delay	1.5000
9	Pulse Width	20.5500
10	Acquisition Time	1.3981
11	Acquisition Date	2019-10-10T14:42:15
12	Modification Date	2019-10-10T14:42:48
13	G to G'	1.00000000
14	Echo Delay	0.0000
15	Gradient Duration	0.0000
16	Spectrometer Frequency	78.22
17	Spectral Width	23437.5
18	Lowest Frequency	-3896.5
19	Nucleus	
20	Acquired Size	32768
21	Spectral Size	65536

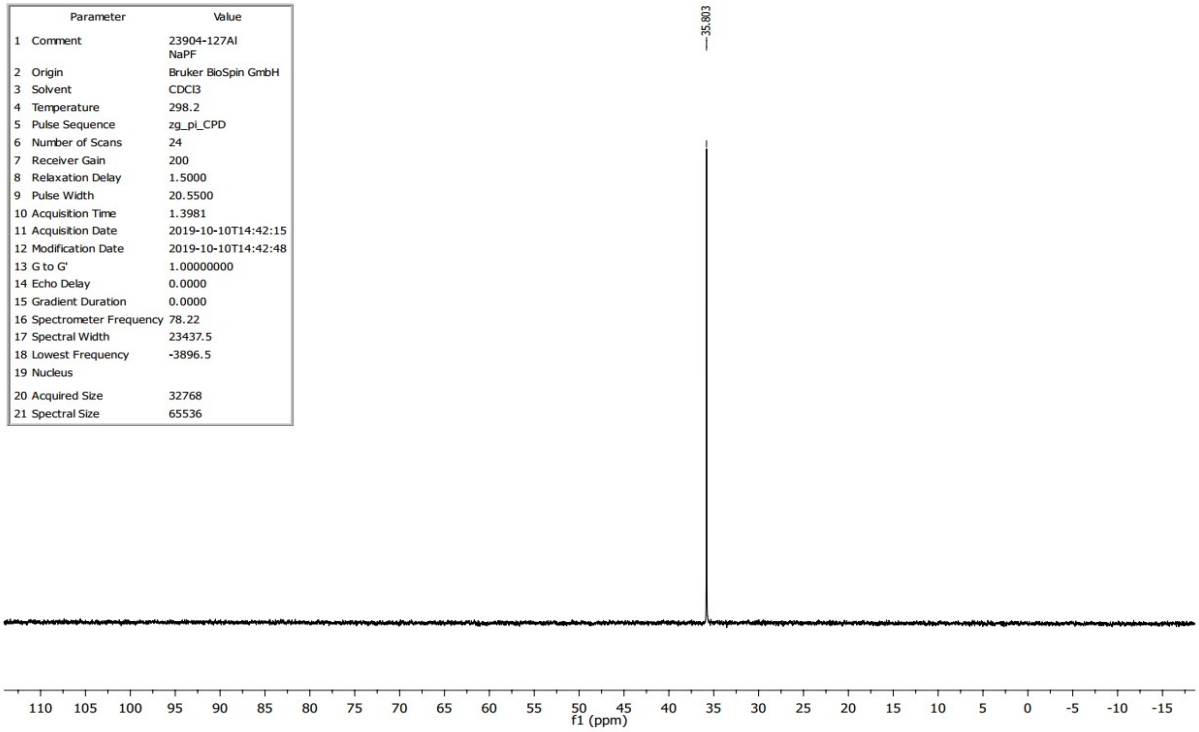

$K[Al(OR^F)_4]$

19F

	Parameter	Value
1	Comment	23905-19F KPF
2	Origin	Bruker BioSpin GmbH
3	Solvent	CD2Cl2
4	Temperature	298.2
5	Pulse Sequence	zg_pi
6	Number of Scans	32
7	Receiver Gain	200
8	Relaxation Delay	0.0000
9	Pulse Width	15.0000
10	Acquisition Time	0.9787
11	Acquisition Date	2019-10-10T14:25:12
12	Modification Date	2019-10-10T14:25:40
13	G to G'	1.00000000
14	Echo Delay	0.0000
15	Gradient Duration	0.0000
16	Spectrometer Frequency	282.47
17	Spectral Width	66964.3
18	Lowest Frequency	-61729.2
19	Nucleus	19F
20	Acquired Size	65536
21	Spectral Size	131072

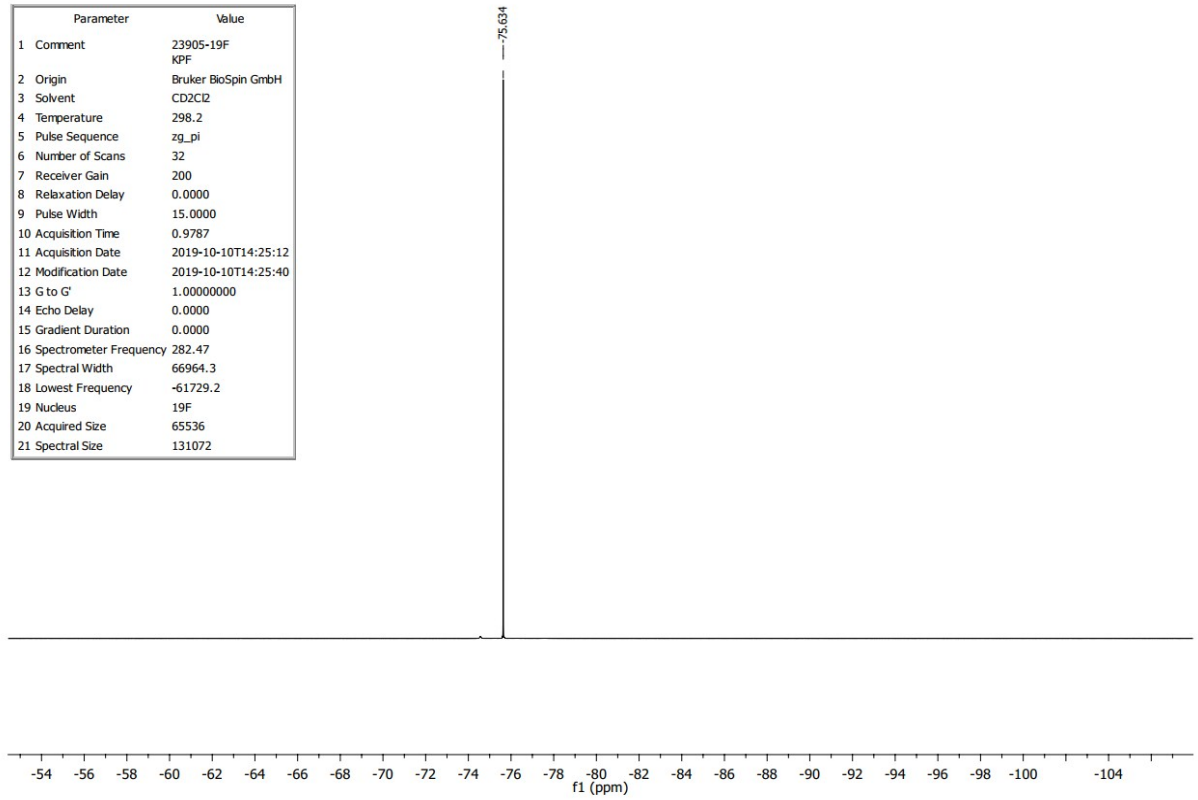

27Al

	Parameter	Value
1	Comment	23905-27Al KPF
2	Origin	Bruker BioSpin GmbH
3	Solvent	CD2Cl2
4	Temperature	298.2
5	Pulse Sequence	zg_pi_CPD
6	Number of Scans	12
7	Receiver Gain	200
8	Relaxation Delay	1.5000
9	Pulse Width	20.5500
10	Acquisition Time	1.3981
11	Acquisition Date	2019-10-10T14:43:57
12	Modification Date	2019-10-10T14:44:27
13	G to G'	1.00000000
14	Echo Delay	0.0000
15	Gradient Duration	0.0000
16	Spectrometer Frequency	78.22
17	Spectral Width	23437.5
18	Lowest Frequency	-3896.5
19	Nucleus	
20	Acquired Size	32768
21	Spectral Size	65536

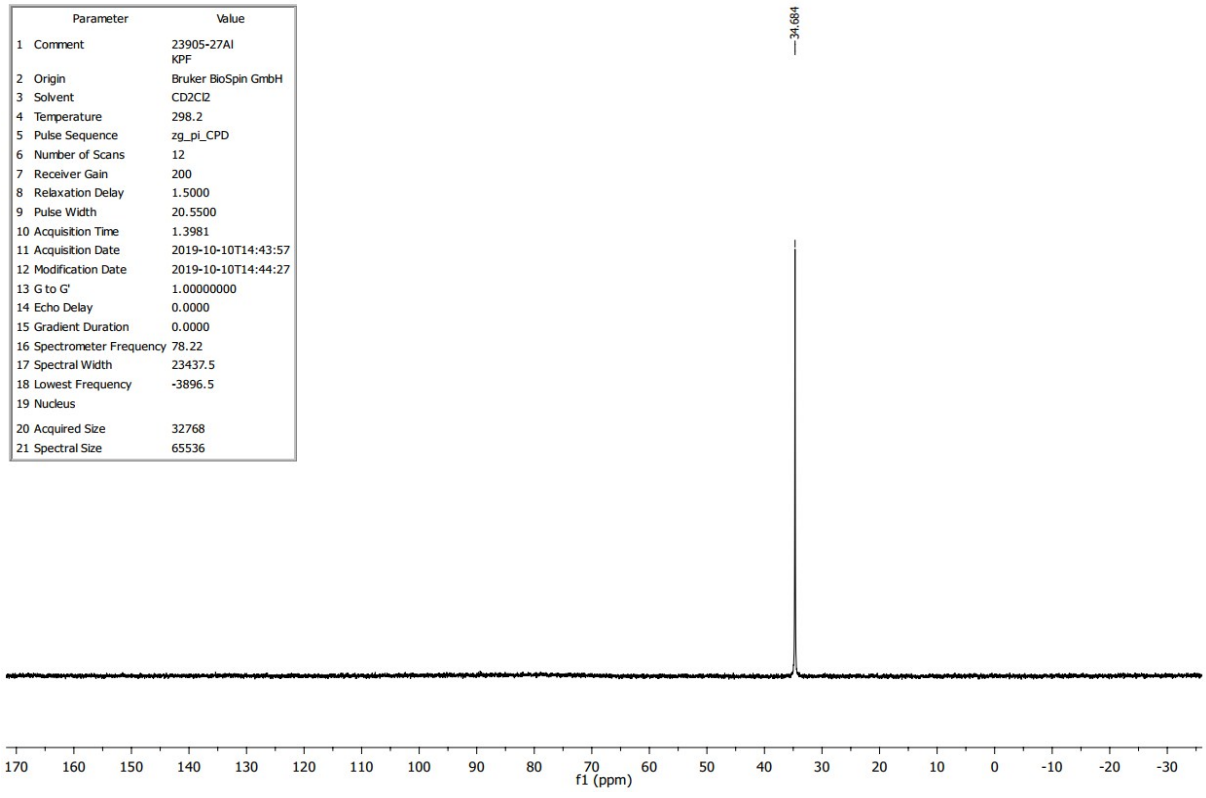

$Rb[Al(OR^F)_4]$

19F

	Parameter	Value
1	Comment	23906-19F RbPF
2	Origin	Bruker BioSpin GmbH
3	Solvent	CD2Cl2
4	Temperature	298.1
5	Pulse Sequence	zg_pi
6	Number of Scans	32
7	Receiver Gain	200
8	Relaxation Delay	0.0000
9	Pulse Width	15.0000
10	Acquisition Time	0.9787
11	Acquisition Date	2019-10-10T14:30:10
12	Modification Date	2019-10-10T14:30:11
13	G to G'	1.00000000
14	Echo Delay	0.0000
15	Gradient Duration	0.0000
16	Spectrometer Frequency	282.44
17	Spectral Width	66964.3
18	Lowest Frequency	-61729.2
19	Nucleus	19F
20	Acquired Size	65536
21	Spectral Size	131072

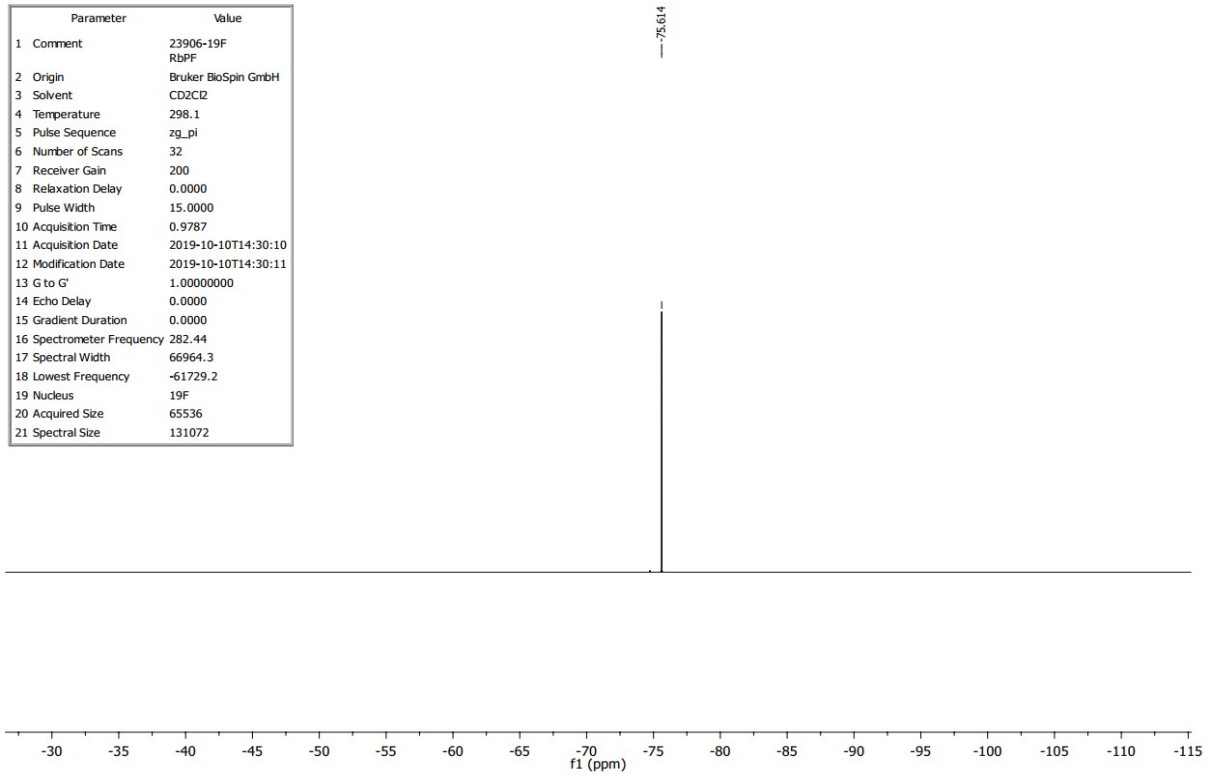

27Al

	Parameter	Value
1	Comment	23906-27Al RbPF
2	Origin	Bruker BioSpin GmbH
3	Solvent	CD2Cl2
4	Temperature	298.2
5	Pulse Sequence	zg_pi_CPD
6	Number of Scans	9
7	Receiver Gain	200
8	Relaxation Delay	1.5000
9	Pulse Width	20.5500
10	Acquisition Time	1.3981
11	Acquisition Date	2019-10-10T14:46:50
12	Modification Date	2019-10-10T14:47:05
13	G to G'	1.00000000
14	Echo Delay	0.0000
15	Gradient Duration	0.0000
16	Spectrometer Frequency	78.22
17	Spectral Width	23437.5
18	Lowest Frequency	-3896.5
19	Nucleus	
20	Acquired Size	32768
21	Spectral Size	65536

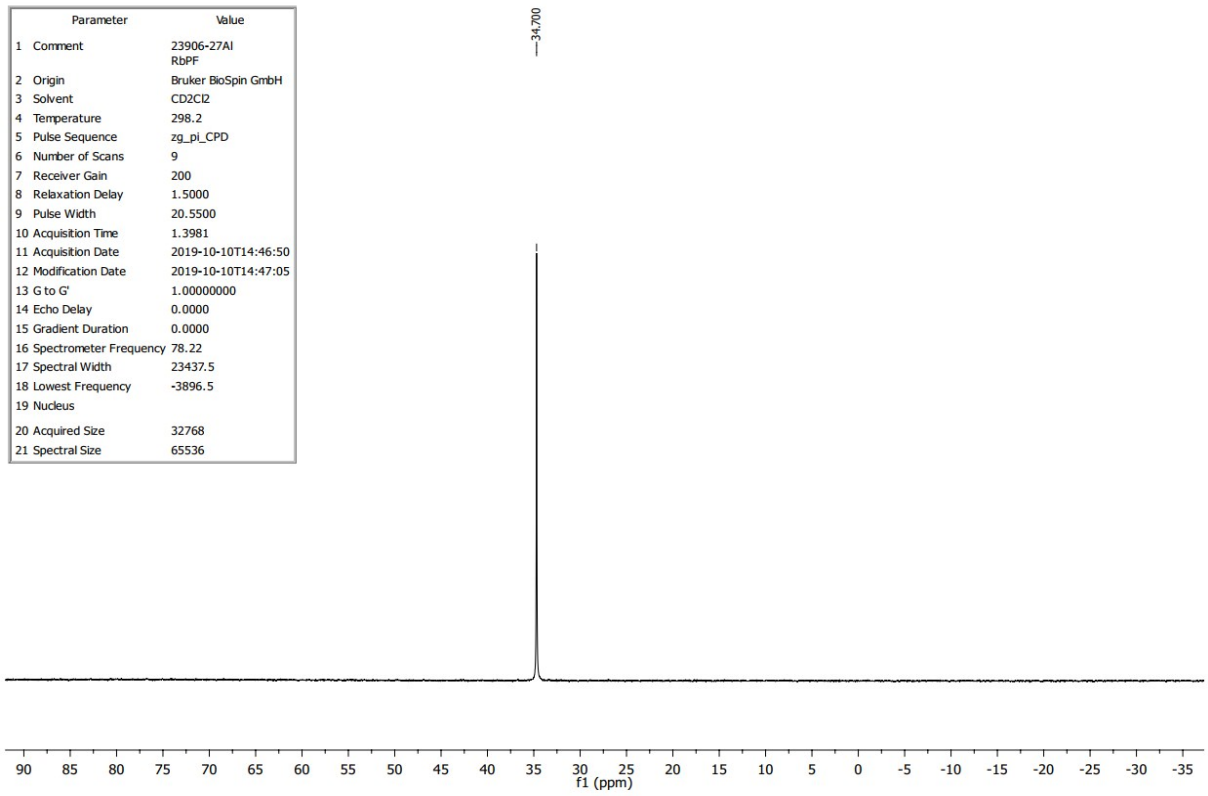

$Cs[Al(OR^F)_4]$

19F

	Parameter	Value
1	Comment	23907-19F CsPF
2	Origin	Bruker BioSpin GmbH
3	Solvent	CD2Cl2
4	Temperature	298.1
5	Pulse Sequence	zg_pi
6	Number of Scans	32
7	Receiver Gain	200
8	Relaxation Delay	0.0000
9	Pulse Width	15.0000
10	Acquisition Time	0.9787
11	Acquisition Date	2019-10-10T14:33:21
12	Modification Date	2019-10-10T14:33:21
13	G to G'	1.00000000
14	Echo Delay	0.0000
15	Gradient Duration	0.0000
16	Spectrometer Frequency	282.47
17	Spectral Width	66964.3
18	Lowest Frequency	-61729.2
19	Nucleus	19F
20	Acquired Size	65536
21	Spectral Size	131072

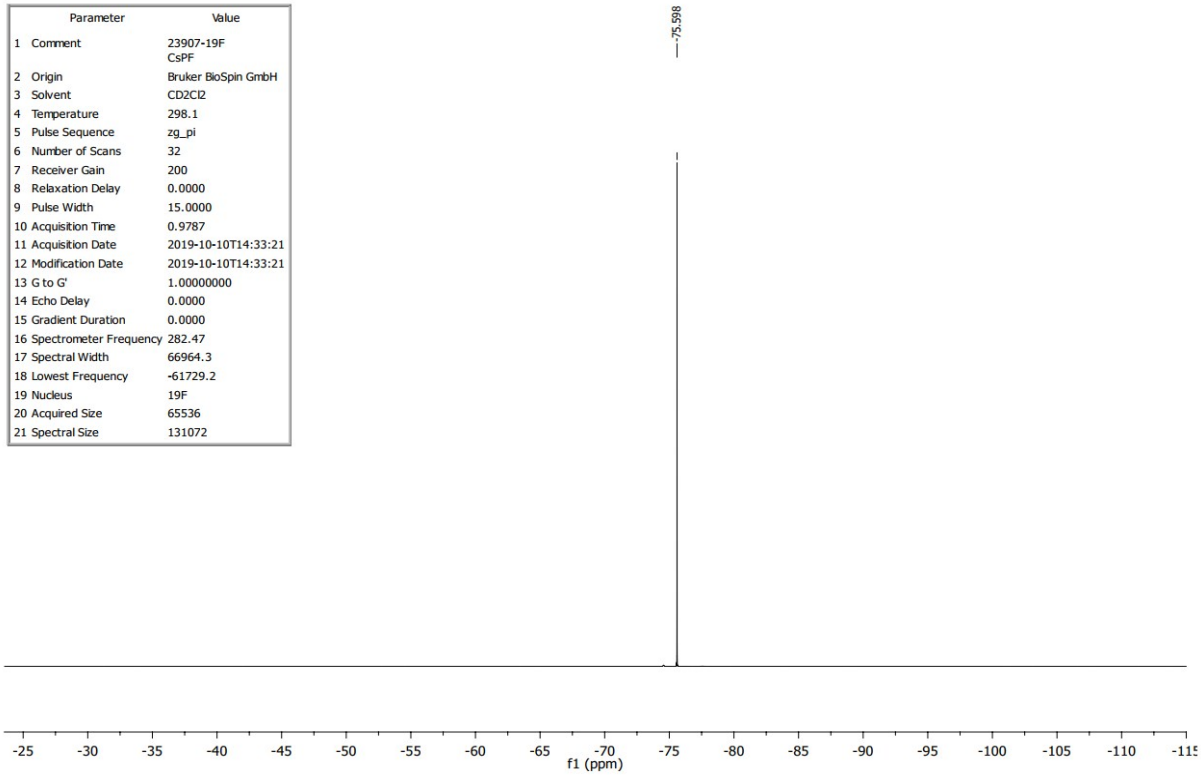

27Al

	Parameter	Value
1	Comment	23907-27Al CsPF
2	Origin	Bruker BioSpin GmbH
3	Solvent	CD2Cl2
4	Temperature	298.2
5	Pulse Sequence	zg_pi_CPD
6	Number of Scans	13
7	Receiver Gain	200
8	Relaxation Delay	1.5000
9	Pulse Width	20.5500
10	Acquisition Time	1.3981
11	Acquisition Date	2019-10-10T14:49:32
12	Modification Date	2019-10-10T14:49:50
13	G to G'	1.00000000
14	Echo Delay	0.0000
15	Gradient Duration	0.0000
16	Spectrometer Frequency	78.22
17	Spectral Width	23437.5
18	Lowest Frequency	-3896.5
19	Nucleus	
20	Acquired Size	32768
21	Spectral Size	65536

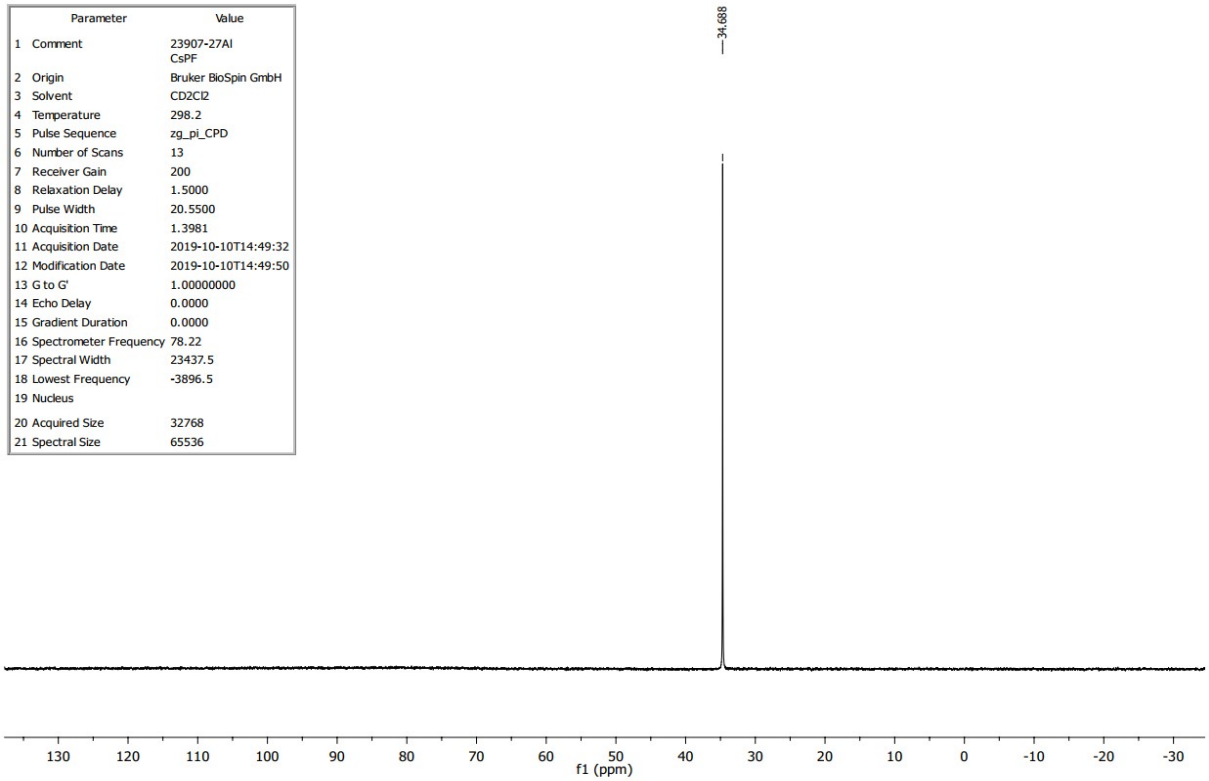

3. Crystallographic data

Table S2. Crystallographic data for refined structures.

Compound	$Li[Al(OR^F)_4]$	$Na[Al(OR^F)_4]$	$K[Al(OR^F)_4]$	$Rb[Al(OR^F)_4]$	$Cs[Al(OR^F)_4]$	$NH_4[Al(OR^F)_4]$	$N_2H_5[Al(OR^F)_4]$	$N_2H_7[Al(OR^F)_4]$	Ag[***alfal***]	Cu[***alfal***]
K_α	0.71073 (Mo)	0.71073 (Mo)	0.71073 (Mo)	0.71073 (Mo)	0.71073 (Mo)	1.54184 (Cu)	1.54184 (Cu)	0.71073 (Mo)	0.71073 (Mo)	1.54184 (Cu)
Temperature (K)	100	190	100	100	100	100	100	100	100	100
Space group	$P2_12_12_1$	$P2_1/c$	$P2_1/c$	$P1$	$P1$	$P1$	$P1$	$P\bar{1}$	$P2_1/c$	$P\bar{1}$
Z	4	4	8	2	4	2	2	8	4	2
a (Å)	9.9680(5)	13.6410(8)	23.8816(11)	9.6213(7)	17.1845(18)	9.6278(4)	9.6450(4)	17.4972(8)	21.151(2)	10.5661(5)
b (Å)	13.4495(6)	10.1222(6)	12.9259(6)	10.4768(7)	17.4964(18)	10.5021(4)	10.6675(5)	17.5074(7)	10.2666(10)	10.7463(4)
c (Å)	21.0791(10)	21.3566(13)	20.6284(10)	16.8127(12)	18.6544(19)	16.8670(4)	17.0803(8)	20.3760(9)	21.257(2)	22.2844(8)
α (°)	90	90	90	81.079(4)	105.940(2)	81.237(3)	82.791(4)	91.583(2)	90	82.600(3)
β (°)	90	89.957(3)	115.546(2)	73.385(3)	105.366(2)	73.421(3)	73.622(4)	91.488(2)	112.868(3)	87.100(3)
γ (°)	90	90	90	62.701(3)	113.601(2)	62.778(4)	63.240(4)	105.979(2)	90	61.460(4)
V (Å^3)	2826.0(2)	2948.9(3)	5745.3(5)	1442.53(18)	4472.2(8)	1453.04(10)	1505.47(13)	5994.7(5)	4253.3(7)	2204.15(17)
$\rho_{calc.}$ (g cm^{-3})	2.290	2.230	2.327	2.423	2.451	2.243	2.201	2.221	2.485	2.333
$\mu_{exp.}$ (mm^{-1})	0.340	0.341	0.480	2.010	1.526	3.163	3.075	0.326	0.801	3.877
ϑ_{max} (°)	27.517	23.2155	26.667	27.658	30.768	72.051	75.288	26.097	28.740	68.252
R_1	2.83%	3.78%	3.30%	2.23%	4.62%	5.64%	4.55%	4.95%	2.90%	7.19%
wR_2	7.37%	10.25%	8.20%	4.77%	10.71%	15.06%	12.08%	12.90%	6.50%	19.46%
GooF	1.156	1.052	1.034	1.036	1.043	1.056	1.039	1.033	1.134	1.026
Crystal size (mm×mm×mm)	0.20x0.30x0.38	0.08x0.08x0.25	0.07x0.15x0.15	0.10x0.12x0.13	0.08x0.10x0.20	0.08x0.14x0.19	0.21x0.28x0.35	0.20x0.23x0.24	0.10x0.25x0.40	0.05x0.12x0.15
Crystal color	colorless	colorless	colorless	colorless	colorless	colorless	colorless	colorless	colorless	colorless
CCDC No.	1960194	1960196	1960195	1960197	1960198	1960459	1960205	1960204	1960514	1960199

4. Supplementary data and figures for description of the crystal structures

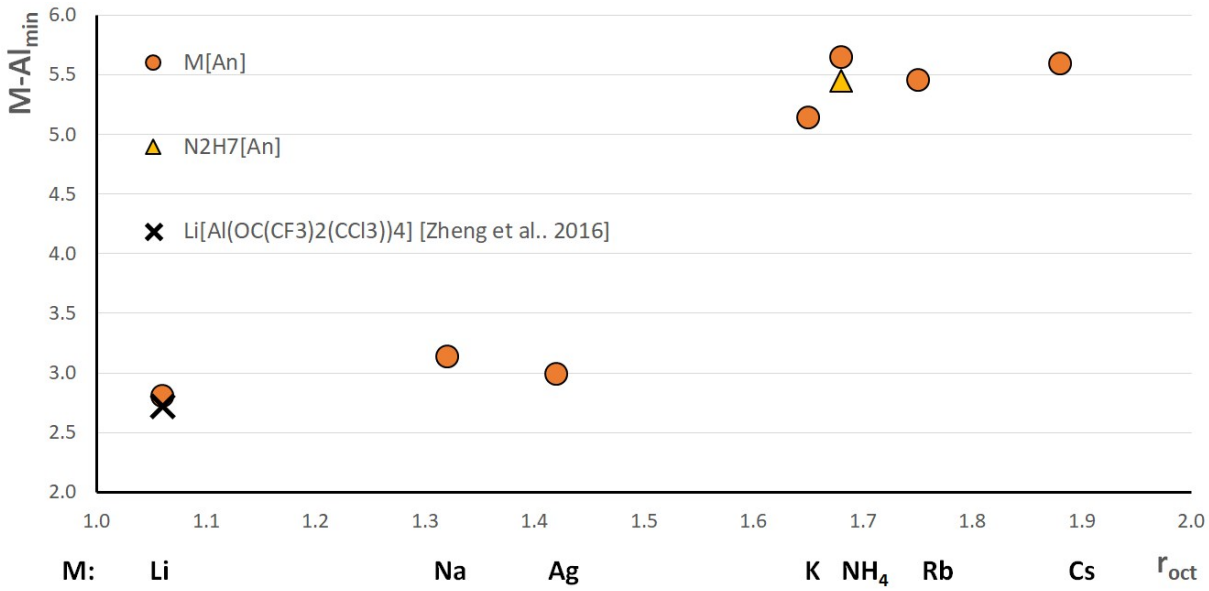

Figure S11. The minimal M–Al distances [Å] observed in the crystals in the function of crystallographic octahedral radii [Å].

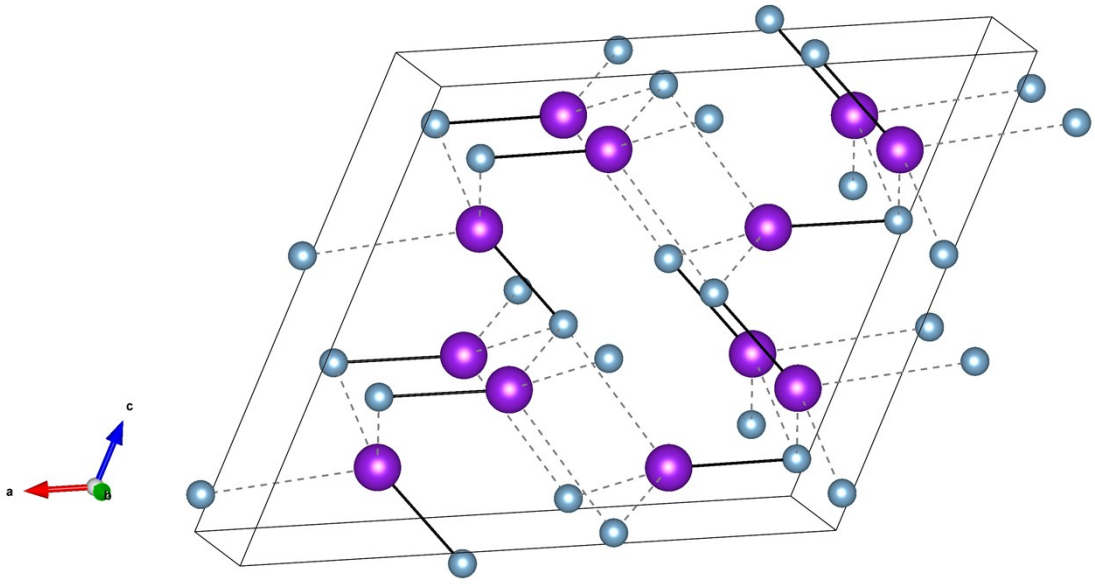

Figure S12. View of KAl sublattice in the crystal structure of K[Al(OR^F)$_4$]. Purple: K, blue: Al. Black solid line: the shortest K-Al distance (*ca.* 5.2 Å), dashed grey lines: K-Al distances in the range of 7 – 8 Å.

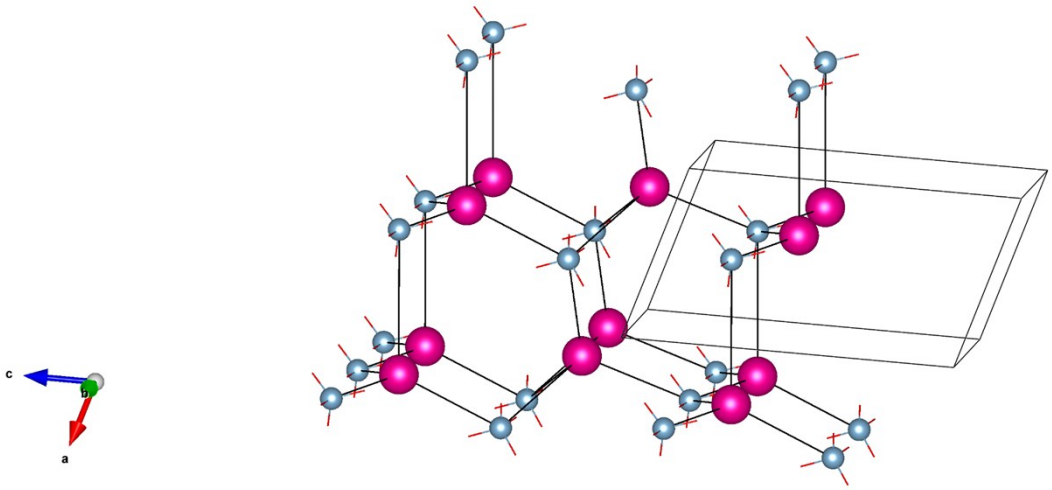

Figure S13. View of RbAl sublattice in the crystal structure of $Rb[Al(OR^F)_4]$. Pink: Rb, blue: Al. Similar arrangement has also been observed for M = Cs and NH_4.

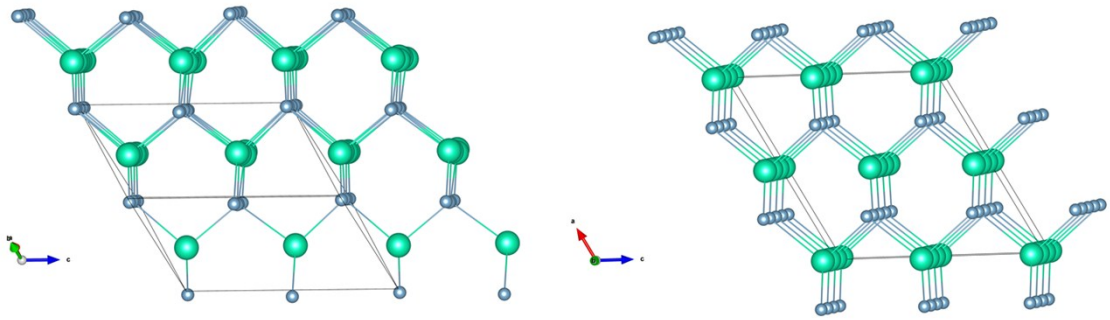

Figure S14. The view of CsAl sublattice in $Cs[Al(OR^F)_4]$ at 100 K (left) and 200 K (right).[S14] The orientation of both structures is set to see the modulation in the arrangement of Cs and Al in the former one. Celadon: Cs, blue: Al.

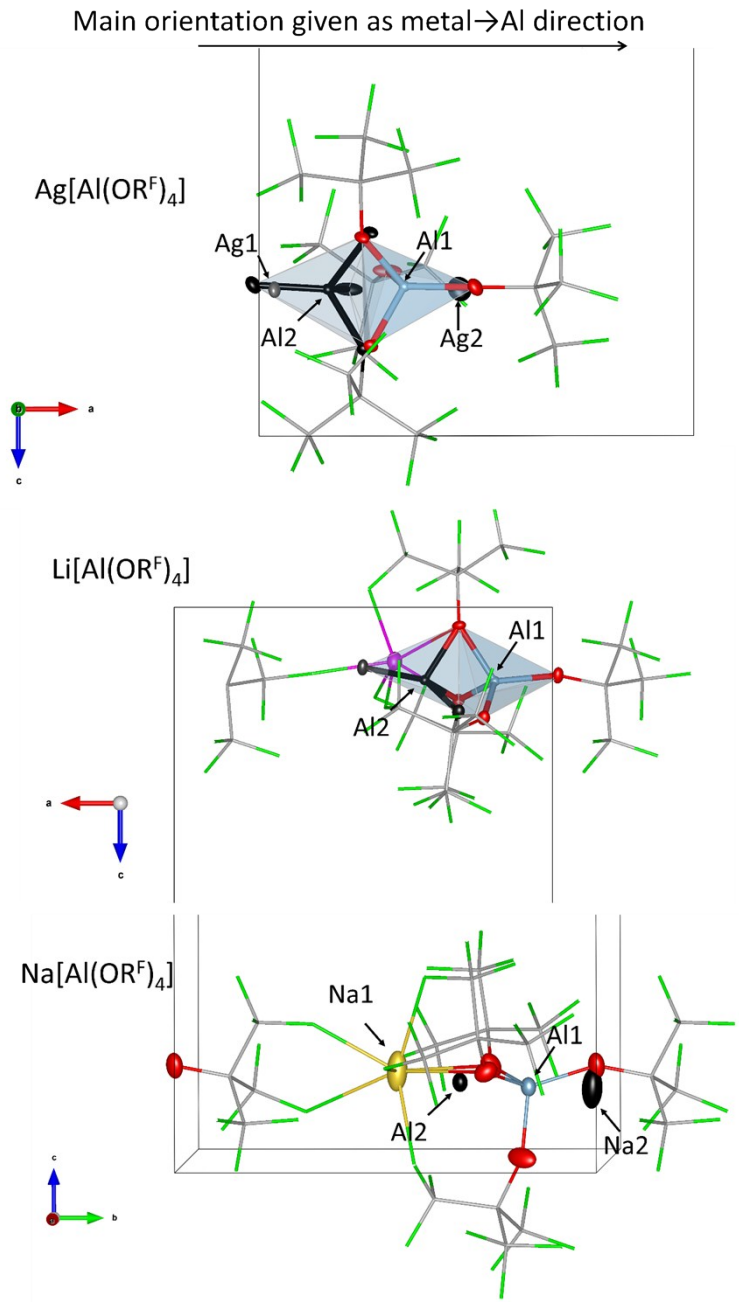

Figure S15. Visualization of the disorder in $\{M[Al(OR^F)_4]\}_\infty$ chains (M=Ag,[S6] Li, Na). The atoms from main orientation are in colour, while localized atoms from the opposite orientation are in black. Disorder in -OR^F groups, thermal ellipsoids of C and F atoms are omitted for clarity.

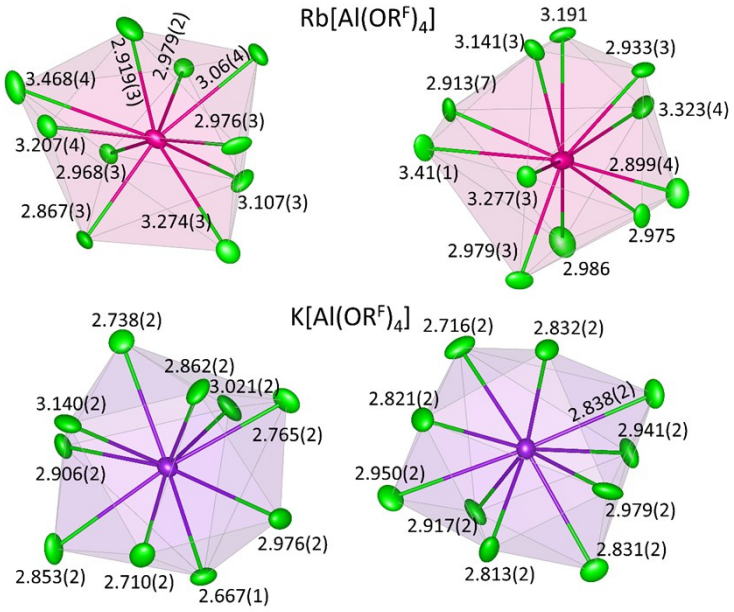

Figure S16. Coordination spheres of K^+ (purple) and Rb^+ (violet) in their $[Al(OR^F)_4]^-$ salts. Bond lengths given in Å.

Cs[Al(OR^F)$_4$]- toluene adduct

Due to the weakly coordinating character and large size of $[Al(OR^F)_4]^-$, even the large Cs^+ is able to form a fairly stable solvate with a toluene molecule. Cs coordinates in η^6-fashion with very long Cs–C distances exceeding 3.44 Å and Cs–aromatic ring distance of ca. 3.2 Å, which are in agreement with the DFT predictions (B3LYP/def2-TZVP/D3BJ). Toluene molecules are arranged in a way that the methyl group is pointing perpendicular to the aromatic ring of its neighbor enabling a CH···π interaction at *ca.* 3.6 Å (see Figure S17), which is the most thermodynamically favored mode of bonding between two methyl-substituted aromatic molecules.[S16] Coordination of the toluene molecules renders the structure layered, if weak toluene-toluene interactions are neglected. On the basis of the DFT calculations, the Cs^+-toluene dissociation energy is $\Delta_r H$ = −50 kJ mol^{-1} and $\Delta_r G$ = −26 kJ mol^{-1}. Based on the Jenkins equation,[S17] the energetic cost of lattice expansion upon toluene coordination is estimated at 15 kJ mol^{-1}. For smaller anions the value is much higher, even higher than the coordination energy. *E.g.*, for the $[SbF_6]^-$ anion, the lattice energy change would be 96 kJ mol^{-1} which significantly outweighs the Cs^+-toluene interaction energy.

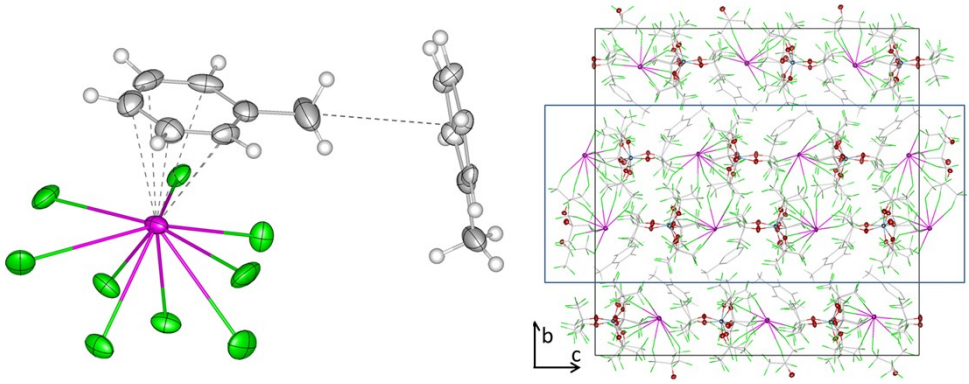

Figure S17. Views of the crystal structure of $Cs(C_6H_5CH_3)[Al(OR^F)_4]$. Left: coordination sphere Cs including the neighbouring toluene molecule; right: the view of the crystal structure along a axis with one layer marked with blue rectangle.

Table S3. Crystallographic data for refined structure of $Cs(C_6H_5CH_3)[Al(OR^F)_4]$.

Compound	$Cs(C_6H_5CH_3)[Al(OR^F)_4]$
K_α	1.54184 (Cu)
Temperature (K)	100
Space group	$P2_1/n$
Z	24
a (Å)	21.7362(2)
b (Å)	31.2247(2)
c (Å)	33.0960(3)
α (°)	90
β (°)	107.8910(10)
γ (°)	90
V (Å^3)	21376.2(3)
$\rho_{calc.}$ (g cm^{-3})	2.219
$\mu_{exp.}$ (mm^{-1})	10.490
ϑ_{max} (°)	76.378
R_1	5.62%
wR_2	14.67%
GooF	1.040
Crystal size (mm×mm×mm)	0.18x0.28x0.78
Crystal colour	colorless
CCDC No.	1960207

5. DFT calculations details and results

All calculations were performed with the use of Orca [S18] (v. 4.0.1.2) using B3LYP [S19] functional with def2-TZVP [S20] (with ECP and Cs [S21]) and D3BJ dispersion correction. [S22] or RIJCOSX [S23] approximation was used to increase the speed of calculations (with auxiliary basis set by Weigend [S24]). Thermal contributions to *ab initio* reaction energies were calculated with inclusion of zero point energy, thermal contributions to the enthalpy/entropy. Graphical presentation of the calculated structures and molecular orbitals has been performed with Avogadro [S25] or Vesta. [S13]

5.1. Coordinates of optimized structures

Cs^+-($C_6H_5CH_3$) **B3LYP/def2-TZVP/D3BJ**

C	-1.55298854709061	1.61409179842090	-0.04665566911667
C	-0.20608824339348	1.99356428661840	-0.07745359924700
C	0.81100572665118	1.04266244038421	-0.03557681375910
C	0.50028052650990	-0.31405854515234	0.03019160427540
C	-0.83573401035016	-0.70813585173784	0.05143341755952
C	-1.84887069630477	0.24739458578233	0.00926648900364
C	-2.64714597310179	2.64568497121835	-0.01375451571669
H	0.04866579178759	3.04671636139091	-0.10226829850079
H	-1.09016765041315	-1.75796012191355	0.12686102378385
H	-2.88405014378278	-0.07044744682498	0.05219688214897
H	1.84537301814381	1.36299570339722	-0.02784861330991
H	1.28895384866559	-1.05252651891820	0.09409778057470
H	-3.57696843451420	2.26222997042325	-0.43467990409583
H	-2.36601345249387	3.55094939473346	-0.55307169253033
H	-2.85751343122056	2.93925334442210	1.01795680008316
Cs	-0.50082832909268	0.47935562775577	-3.29031489115291

$C_6H_5CH_3$ **B3LYP/def2-TZVP/D3BJ**

C	-1.56473879485697	1.60774051209632	-0.00000060859449
C	-0.22104914807202	1.98848970594859	-0.00000013724249
C	0.79134895610879	1.03881432155158	-0.00000041596318
C	0.47872739722706	-0.31696655760333	0.00000005844254
C	-0.85301333439763	-0.70996555053212	0.00000004087133
C	-1.86344060025997	0.24631764384811	-0.00000009618781
C	-2.65422905045620	2.64634761350377	0.00000006854494
H	0.03266457309567	3.04260278663147	-0.00000031120099
H	-1.10868714874082	-1.76223479471793	-0.00000009025738
H	-2.90020905433412	-0.06948144684968	-0.00000026859002
H	1.82661358237225	1.35648194574242	-0.00000020332523
H	1.26728025610395	-1.05850675097700	0.00000109099985
H	-3.64184563261802	2.18480277117256	-0.00000001390742
H	-2.58495116310355	3.29131440698536	-0.87942732209739
H	-2.58495083806842	3.29131339319989	0.87942820850772

NH_4^+ **B3LYP/def2-TZVP/D3BJ**

N	-0.23246307446417	0.29429869463271	-0.01004821075834
H	0.79068791738210	0.35145441389858	0.01998959538056
H	-0.60507467633292	1.10204210931161	-0.51978309021493
H	-0.60240885798735	0.29248188771124	0.94594013442097
H	-0.51296130859766	-0.56897710555414	-0.48666842882826

$N_2H_7^+$ B3LYP/def2-TZVP/D3BJ

H	0.80705538373505	0.43776681029806	-0.02046926157133
H	-0.79392503946007	1.05049396841255	-0.52565093785329
H	-0.68823392063696	0.30869378474451	0.95003006130973
H	-0.59608200858890	-0.58974604736335	-0.43640375314408
N	2.32231603527584	0.62285109196387	-0.03738003095423
H	2.59901548585837	1.56193481690543	0.24202493396214
H	2.79613877813952	-0.02034697843149	0.59368535997936
H	2.71711341699923	0.46629399078629	-0.96269284400600

HCl B3LYP/def2-TZVP/D3BJ

Cl	1.24106490345696	0.00000000000000	0.00000000000000
H	-0.04106490345696	0.00000000000000	0.00000000000000

NH_4Cl B3LYP/def2-TZVP/D3BJ

N	-0.16900093693308	0.05368279604144	0.11435838027586
H	0.75504079510498	-0.32742093760746	0.28592581935059
H	-0.04950577236071	1.69801426839939	-0.50004793241511
H	-0.68273031212324	0.04167455378346	0.98848725242791
H	-0.64533956069071	-0.55576592205614	-0.54143649794028
Cl	0.05187578700275	2.95522524143931	-0.95010702169896

Supplementary references

[S1] I. Krossing, A. Reisinger, *Coord. Chem. Rev.*, **2006**, *250*, 2721–2744.

[S2] M. G. Freire, L. Gomes, L. M. N. B. F. Santos, I. M. Marrucho, J. A. P. Coutinho, *J. Phys. Chem. B* **2006**, *110*, 22923–22929.

[S3] I. K. I. Raabe, A. Reisinger, in *Experiments in Green and Sustainable Chemistry (Eds. H. W. Roesky, D. K. Kennepohl)*, Wiley-VCH, Weinheim, 2009, pp. 131–144.

[S4] J. A. Dilts, E. C. Ashby, *Inorg. Chem.* **1972**, *11*, 1230–1236.

[S5] T. Jaroń, P. A. Orłowski, W. Wegner, K. J. Fijałkowski, P. J. Leszczyński and W. Grochala, *Angew. Chem. Int. Ed.*, 2015, **54**, 1236–1239.

[S6] P. J. Malinowski, D. Himmel and I. Krossing, *Angew. Chemie Int. Ed.*, 2016, **55**, 9259–9261.

[S7] T. A. Engesser, C. Friedmann, A. Martens, D. Kratzert, P. J. Malinowski, I. Krossing, *Chem. Eur. J.* **2016**, *22*, 15085–15094.

[S8] A. Martens, P. Weis, M. C. Krummer, M. Kreuzer, A. Meierhöfer, S. C. Meier, J. Bohnenberger, H. Scherer, I. Riddlestone, I. Krossing, *Chem. Sci.* **2018**, *9*, 7058–7068.

[S9] Agilent (2014). *CrysAlis PRO*. Agilent Technologies Ltd, Yarnton, Oxfordshire, England.

[S10] G. M. Sheldrick, *Acta Cryst.* **2015**, *A71*, 3–8.

[S11] C. B. Hübschle, G. M. Sheldrick, B. Dittrich, *J. Appl. Crystallogr.* **2011**, *44*, 1281–1284.

[S12] D. Kratzert, J. J. Holstein, I. Krossing, *J. Appl. Crystallogr.* **2015**, *48*, 933–938.

[S13] K. Momma, F. Izumi, *J. Appl. Crystallogr.* **2011**, *44*, 1272–1276.

[S14] I. Krossing, H. Brands, R. Feuerhake, S. Koenig, *J. Fluorine Chem.* **2001**, *112*, 83–90.

[S15] I. Raabe, K. Wagner, K. Guttsche, M. Wang, M. Grätzel, G. Santiso-Quiñones, I. Krossing, *Chem. Eur. J.* **2009**, *15*, 1966–1976.

[S16] C. R. Martinez and B. L. Iverson, *Chem. Sci.*, 2012, **3**, 2191.

[S17] H. D. B. Jenkins, H. K. Roobottom, J. Passmore and L. Glasser, *Inorg. Chem.*, 1999, **38**, 3609–3620.

[S18] F. Neese, *WIREs Comput. Mol. Sci.* **2018**, e1327.

[S19] a) A. D. Becke, *J. Chem. Phys.* **1993**, *98*, 5648–5652; b) C. Lee, W. Yang, R. G. Parr, *Phys. Rev. B* **1988**, *37*, 785–789; c) P. J. Stephens, F. J. Devlin, C. F. Chabalowski, M. J. Frisch, *J. Phys. Chem.* **1994**, *98*, 11623–11627.

[S20] a) F. Weigend, M. Häser, H. Patzelt, R. Ahlrichs, *Chem. Phys. Lett.* **1998**, *294*, 143–152; b) F. Weigend, R. Ahlrichs, *Phys. Chem. Chem. Phys.* **2005**, *7*, 3297–3305.

[S21] T. Leininger, A. Nicklass, W. Kuechle, H. Stoll, M. Dolg, A. Bergner, *Chem. Phys. Lett.* **1996**, *255*, 274–280.
[S22] S. Grimme, S. Ehrlich, L. Goerigk, *J. Comput. Chem.* **2011**, *32*, 1456-1465.
[S23] F. Neese, F. Wennmohs, A. Hansen, U. Becker, *Chem. Phys.* **2009**, *356*, 98–109.
[S24] F. Weigend, *Phys. Chem. Chem. Phys.* **2006**, *8*, 1057–1065.
[S25] a) Avogadro: an open-source molecular builder and visualization tool. Version 1.1.1. http://avogadro.cc/ ; b) M. D. Hanwell; D. E. Curtis, D. C. Lonie, T. Vandermeersch, E. Zurek, G. E. Hutchison, *J. Cheminform.* **2012**, 4:17.